UNCLASSIFIED

AD NUMBER
AD380954
CLASSIFICATION CHANGES
TO: unclassified
FROM: confidential
LIMITATION CHANGES
TO: Approved for public release, distribution unlimited
FROM: Distribution authorized to U.S. Gov't. agencies and their contractors; Administrative/Operational Use; APR 1967. Other requests shall be referred to Office of Naval Research, Arlington, VA 22203.
AUTHORITY
30 Apr 1979, DoDD 5200.10; ONR ltr, 15 Jun 1979

THIS PAGE IS UNCLASSIFIED

AD 380954

Technical Report 3

April 1967

THE APPLICATION OF SEISMOMETERS TO ARCTIC ASW — AN ANALYTICAL STUDY (U)

Prepared for:

SUBMARINE ARCTIC WARFARE AND SCIENTIFIC PROGRAM
NAVAL ORDINANCE LABORATORY
WHITE OAK, MARYLAND

CONTRACT Nonr-2332(00)

STANFORD RESEARCH INSTITUTE

MENLO PARK, CALIFORNIA

SRI

STANFORD RESEARCH INSTITUTE
MENLO PARK, CALIFORNIA

NAVAL WARFARE RESEARCH CENTER April 1967

Technical Report 3

THE APPLICATION OF SEISMOMETERS TO ARCTIC ASW — AN ANALYTICAL STUDY (U)

Prepared for:

SUBMARINE ARCTIC WARFARE AND SCIENTIFIC PROGRAM
NAVAL ORDNANCE LABORATORY
WHITE OAK, MARYLAND

CONTRACT Nonr-2332(00)

By: NORMAN E. GOLDSTEIN

SRI Project ETU-2167-612

Approved: E. C. WOOD, MANAGER
GEOPHYSICS DEPARTMENT PHYSICS DIVISION

This document contains information affecting the national defense of the United States within the meaning of the Espionage Laws, Title 18, U.S.C., Sections 793 and 794. Its transmission or the revelation of its contents in any manner to an unauthorized person is prohibited by law.

In addition to security requirements which must be met, this document is subject to special export controls and each transmittal to foreign governments or foreign nationals may be made only with prior approval of Office of Naval Research (Code 462).

SRI-66-3252
2167-612

GROUP-4
DOWNGRADED AT 3-YEAR INTERVALS;
DECLASSIFIED AFTER 12 YEARS

~~Copy No.~~ ....

CONFIDENTIAL

ABSTRACT

In ice-covered waters the usefulness of hydrophones is limited by the necessity to create or to locate openings through which the sensors can enter the water. But ability to detect submarines in Arctic waters is important. For this reason the effectiveness of an on-ice sensor, namely, the geophone, has been studied analytically toward the assessment of its feasibility. Comparisons were made between meager measurements of ice noise reported in the literature and signal levels calculated from normal mode theory. The studies indicate that a submarine emitting one-watt or more at 7 or 8 Hz, a frequency range of low natural noise, might be detectable at a range of 1 km and possibly as large as 30 km.

Noise data is lacking particularly for shallow water areas, where the geophone seems most useful, and experimental measurements are recommended using three component geophones.

No matter what the signal-to-noise ratio, array processing can be used to enhance the probability of recognizing a submarine. However, the acoustic environment causes dispersive waves and this would add to the operational difficulties.

CONTENTS

Nomenclature v

Introduction 1

Basic Theory of a Geophone 2

Natural Particle Velocities of Arctic Ice 4

The Propagation of Sound in the Arctic Ocean and Shallow Arctic Waters 7

Comparison of Signal and Noise Amplitudes on the Surface of an Idealized Arctic Ocean 15

Comparison of Signal and Noise Amplitudes on the Surface of an Idealized Shallow Water Arctic Environment. 24

Comparison of Hydrophone and Geophone Signal-to-Noise Ratios 29

Recognition and Localization of the Source 33

The Use of On-Ice Sensors Other than Geophones 35

Conclusions and Recommendations 36

Appendix A 39

Appendix B 42

Bibliography 44

TABLES

1. The Approximation for the Deep Water Environment 15

2. The Approximation for the Shallow Water Environment 25

ILLUSTRATIONS

Fig. 1 Commercial moving coil seismometer 3

Fig. 2 Ambient vertical particle velocity of Arctic ice 5

Fig. 3 Velocity and density variation in the central Arctic Ocean . 7

Fig. 4 Calculated phase velocity dispersion of guided waves in deep Arctic water 16

Fig. 5 Calculated relative excitation strengths of a few modes for various source depths in deep Arctic water 17

Fig. 6 Vertical particle velocity as a function of range for various source depths (Three Modes, 25 Hz) 18

Fig. 7 Averaged vertical particle velocities of 25-Hz natural ice vibration, 26 April to 14 May, (After Prentiss et al, 1965). 19

Fig. 8 Vertical particle velocity as a function of range for various source depths (Six Modes, 50 Hz, ice bottom irregularities ignored). 20

Fig. 9 Vertical particle velocity as a function of range: 50-Hz output, source depth 25 meters (6 modes) 21

Fig. 10 Vertical particle velocity as a function of range: 100-Hz output, source depth 25 meters (11 modes) 22

Fig. 11 Vertical particle velocity as a function of range: 100-Hz output, source depth 50 meters (11 modes) 23

Fig. 12 Calculated phase velocity dispersion of guided waves in shallow Arctic water. 25

Fig. 13 Excitation strength of first 10 normal modes in shallow Arctic water, source depth 25 meters 26

Fig. 14 Excitation strength of first 10 normal modes in shallow Arctic water, source depth 50 meters 26

Fig. 15 Vertical particle velocity as a function of range, shallow Arctic water, 20-Hz output 28

Fig. 16 Vertical particle velocity as a function of range, shallow Arctic water, 50-Hz output 30

Fig. 17 Vertical particle velocity as a function of range, shallow Arctic water, 100-Hz output 31

Fig. 18 Comparison f hydrophone to geophone signal-to-noise ratio for signals received from distant explosions (after Greene, Elbert, Fitzpatrick, 1966) 32

NOMENCLATURE

e	voltage
y	displacement
ω	circular frequency
ω_N	natural frequency
h	damping factor of a geophone or a layer thickness
h_i	thickness of i-th layer
G	intrinsic sensitivity of a geophone
k	wave number
α_i	compressional wave velocity in the i-th layer of a multilayered acoustical environment
m	mode number, an integer
$\vec{n}_m$	unit vector in the direction of propagation for the m-th mode
$\vec{z}$	unit vector in the vertical direction
k_{mz}	projection of $\vec{n}_m k$ in the vertical direction
k_{mr}	projection of $\vec{n}_m k$ in the horizontal direction, the eigen wavenumber
$\varkappa_{mr}$	complex valued eigen wavenumber
ϵ_{mr}	imaginary part of $\varkappa_{mr}$
V_z	vertical component of particle velocity
V_r	horizontal component of particle velocity
R	horizontal distance between source and receiver
Z	depth of receiver
Z'	depth of source

t time

M maximum mode that may exist for a given frequency

D_m radial term in the expression for particle velocity, m-th mode

F_m vertical term in the expression for particle velocity, m-th mode

W_m excitation function for the m-th mode

P power output of the source

ρ_i density of the i-th layer

L_m a function that relates W_m to the physical layering of an inhomogeneous acoustical environment, m-th mode

c_m phase velocity of the n-th mode

c phase velocity in general

$\chi\uparrow$ phase change occurring for an up-going wave reflected at an interface

$\chi\downarrow$ phase change occurring for a down-going wave reflected at an interface

γ_i value of the eigen wave number in the i-th layer

A_m amplitude of the m-th mode before reflection

A_m' amplitude of the m-th mode after reflection

σ standard deviation of a random surface that has a Gaussian distribution function

$\zeta(x)$ height of the random surface at point x

n number of reflections in distance R

θ_m angle of incidence of m-th mode

Introduction

In the Arctic and Subarctic regions an ice cover would interfere with the use of hydrophones for the detection and location of submarines. To use air-dropped ASW hydrophone systems in ice-covered waters, either a lead must be found or a hole must be made in the ice through which the hydrophone can enter the water. Either task is time consuming. Moreover, leads may not always be found in the area of interest and, unless an area of thin ice is present entry, to the water may be prohibitively difficult.

To overcome the disadvantages of hydrophone installation in ice-covered regions, we have considered the use of seismometers as suitable on-ice sensors (Goldstein 1966). The modern seismometer, or geophone as the small, high-frequency types are called, produces a voltage output whose amplitude depends on the particle motion of the medium to which the transducer is coupled. Because the acoustical energy from an underwater sound source is transmitted as a disturbance in particle motion of the surrounding media, sensitive geophones located on the ice near the source should sense the variations of ice motion.

The modern geophone, a moving-coil transducer, is particularly sensitive to motion in the 1 to 100 Hz range—the bandwidth in which most submersible craft radiate a good portion of acoustical energy. These transducers are rugged, dependable and fairly low in cost, the cost increasing with sensitivity of the device. Their low cost allows them to be considered as expendable items. Furthermore, their ruggedness has already been exploited in the design of an air-droppable seismic surveillance device manufactured for military purposes by R-I Controls, Inc. of Minneapolis, Minnesota.

The effectiveness of on-ice transducers for ASW work has never been evaluated by experiment. However, a limited effort by geophysicists has been directed toward the measurement of natural ice vibration in the Arctic Ocean. The data are relatively meager, but meager as they are they provide us with basic input for an anlytical study.

In the analytical study reported here we have attempted to estimate quantitatively the signal-to-noise ratio resulting from a submarine beneath Arctic ice. The signal amplitudes were evaluated numerically by normal mode

theory with the assumption of a point source radiator. Amplitudes of the noise, or natural vibration, were taken from data reported in the literature. The signal-to-noise ratio was considered for two acoustical environments: deep waters such as the central Arctic Ocean, and shallow water such as continental shelf areas which are deep enough for a submerged fleet-class submarine but may have a seasonal ice cover.

Basic Theory of a Geophone

Most seismometers, except for a few special devices, basically consist of a mass suspended by springs or hinges so that the mass will remain more or less fixed as the frame of suspension moves with the motion of the ground (or ice in our case). Sensed is the relative motion between the mass and the frame.

Seismometers are manufactured for sensing ground motion with periods from one hour to periods as short as 0.005 second. For the detection of nearby natural and artificial disturbances, seismometers with natural frequencies of 1 to 30 Hz are used. These devices, commonly called geophones, will be discussed in this section.

Geophones are small, rugged, and simple in principle (Fig. 1). When coupled to a dynamic medium the transducer's case moves, and a relative motion is set up between a magnet fixed to the case and an internal spring-supported mass on which a conducting coil is wound. Neglecting phase changes, hysteresis, eddy currents, etc., the voltage induced in the coil is proportional to the time rate at which the coil cuts the magnetic lines of force. The expression for voltage so generated can be derived from the equation of motion of a damped linear oscillator and Faraday's law of induction:

$$\ddot{e} + 2h\omega_N \dot{e} + \omega_N^2 e = \dddot{y}G \qquad (1)$$

where

e = voltage output

h = damping term

ω_N = natural frequency of the mechanical system

y = case displacement

G = intrinsic sensitivy

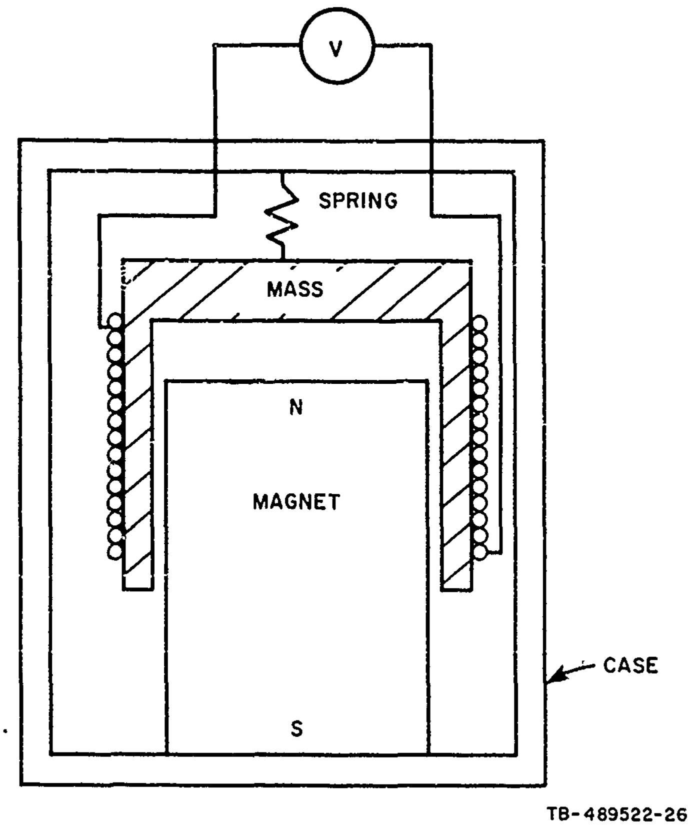

FIG. 1 COMMERCIAL MOVING COIL SEISMOMETER

The dots mean time derivatives. G, the intrinsic sensitivity, is proportional to the number of turns on the coil, the dipole moment of the magnet, and the mass. Because the power output is proportional to mass, the voltage output, hence sensitivity, is proportional to the square root of the mass. Geophones with extremely high sensitivity have masses of a kg or more. Damping, h, between the mass and the frame is required so that the instrument does not oscillate freely when excited.

Two limiting cases of Eq. 1 are of interest for they point out important characteristics of a geophone. When the natural frequency is much less than the excitation frequency, Eq. 1 may be reduced to

$$\dot{e} = \dot{y}G \quad (\omega_N \ll \omega)$$

From this we see that the voltage output is proportional to the velocity of the case and thus the particle velocity of the medium. In this situation the geophone behaves as a velocity gage. On the other hand a different prime characteristic is revealed when the natural frequency is much larger than the excitation frequency. Then Eq. 1 may be approximated by

$$e = \dddot{y}G/\omega_N^2 \quad (\omega_N \gg \omega)$$

and the voltage output, although small, is proportional to the third derivative of particle displacement. Thus for excitation near frequencies of maximum geophone sensitivity ($\omega \sim \omega_N$) the voltage generated will have a complex relation to ground motion: the voltage output will be a superposition of particle velocity and acceleration effects.

This behavior is not detrimental to most geophone applications. If we are interested in knowing only whether or not a disturbance occurs, we need not translate the observed voltage into absolute quantities of ground motion. Our only concern is to choose a transducer with a natural frequency near the frequency of maximum excitation expected. However, calibration tests can be made so that a conversion between voltage and velocity (or displacement) is possible.

Natural Particle Velocities of Arctic Ice

Recent experiments have shown that Arctic ice is in continuous horizontal and vertical motion. In this report we shall consider only the vertical particle velocity of the ice because it is the only component of velocity that has been measured over long periods of time. Fortunately, particle velocities induced in thin ice from an underwater low-frequency sound source are theoretically in the vertical direction (Goldstein, 1966).

Figure 2 shows the amplitude spectra of vertical particle velocity of

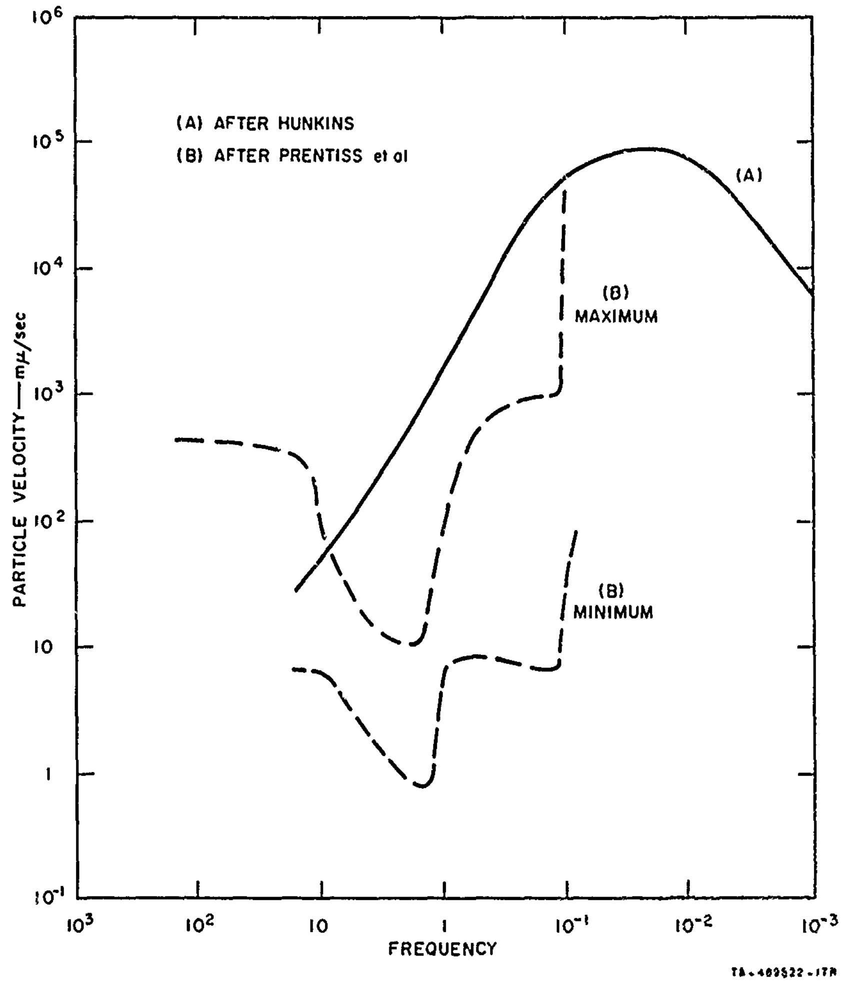

FIG. 2 AMBIENT VERTICAL PARTICLE VELOCITY OF ARCTIC ICE

Arctic ice as determined by Hunkins (1962) and Prentiss, et al (1965). These spectra are plotted in the conventional units used by seismologists: millimicrons per second (mμ/sec) where 1 mμ = 10^{-9} meters. The general characteristics of the observed spectra are a decrease of particle velocity with increasing frequency, a minimum velocity in the frequency range of one to five Hz, and a wide range between minimum and maximum noise intensities over the 10^{-1} to 10^{2} Hz bandwidth. The spectra shown were obtained from observations made on ice over the deeper portions of the Arctic Ocean where the water depth is 2.5 to 2.8 km. This environment qualification of the spectra shown is judged to be important because the

noise spectra depend on the physical properties of the coupled ice-to-sea-water-to-sea-bottom acoustical system. For example, Milne and Clark (1964) reported that closely spaced resonances in seismic background noise in the band 0.1 to 2.0 Hz were observed at the bottom of ice-covered estuaries of the Canadian Arctic where the measured water depth was 0.48 km. These resonances could be explained as the result of multiple internal reflections of plane waves within a layered medium with acoustical properties found from seismic experiments.

During periods of minimum noise the particle velocity of the ice is as small as observed at a quiet continental site. This was first pointed out by Prentiss, et al (1965) who compared their observations of Arctic ice displacements to the continental crust displacements given by Brune and Oliver (1959). During periods of maximum disturbance the particle velocity of Arctic ice will be several hundred $m\mu$/sec, sufficient to completely overwhelm the signal from a nearby underwater source radiating a few watts of acoustic power.

The exact causality between physical processes and natural ice vibrations is not clear, but Arctic researchers have been able to identify a number of general causes for the vibrations. Foremost is wind action. The wind is responsible for much of the low frequency (less than 10^{-2} Hz) bobbing of the sea ice (Prentiss, et al, 1965), the noise above 1 Hz coming from impacts between adjacent floes, and for the motion of granular snow on the ice surface (Milne and Ganton, 1964).

Temperature variations also seem to affect the level of natural vibration amplitudes. During the winter months the falling air temperature late in the afternoon is accompanied by an increasing vibration noise level. This is attributed to ice cracking as a result of increased tensile stresses (Milne and Ganton, 1964).

The particle velocities of the natural vibration have a seasonal variation, the average velocity amplitude being larger in the winter than in the late sumner (Milne and Ganton, 1964; Mellen and Marsh, 1965). In the late summer the ice cover becomes broken and "fluidized", conditions which make the ice a poor generator of noise (Mellen and Marsh, 1965) and a poor transmission medium for ice vibrations.

The Propagation of Sound in the Arctic Ocean and Shallow Arctic Waters

In the ice-covered Arctic Ocean the propagation velocity of acoustic waves in the water increases bilinearly with depth beneath the ice cover. Figure 3 shows the measured variation in propagation velocity and density in the Arctic Ocean. For the crustal portion, the data are based on seismic refraction surveys in the Bering Sea.

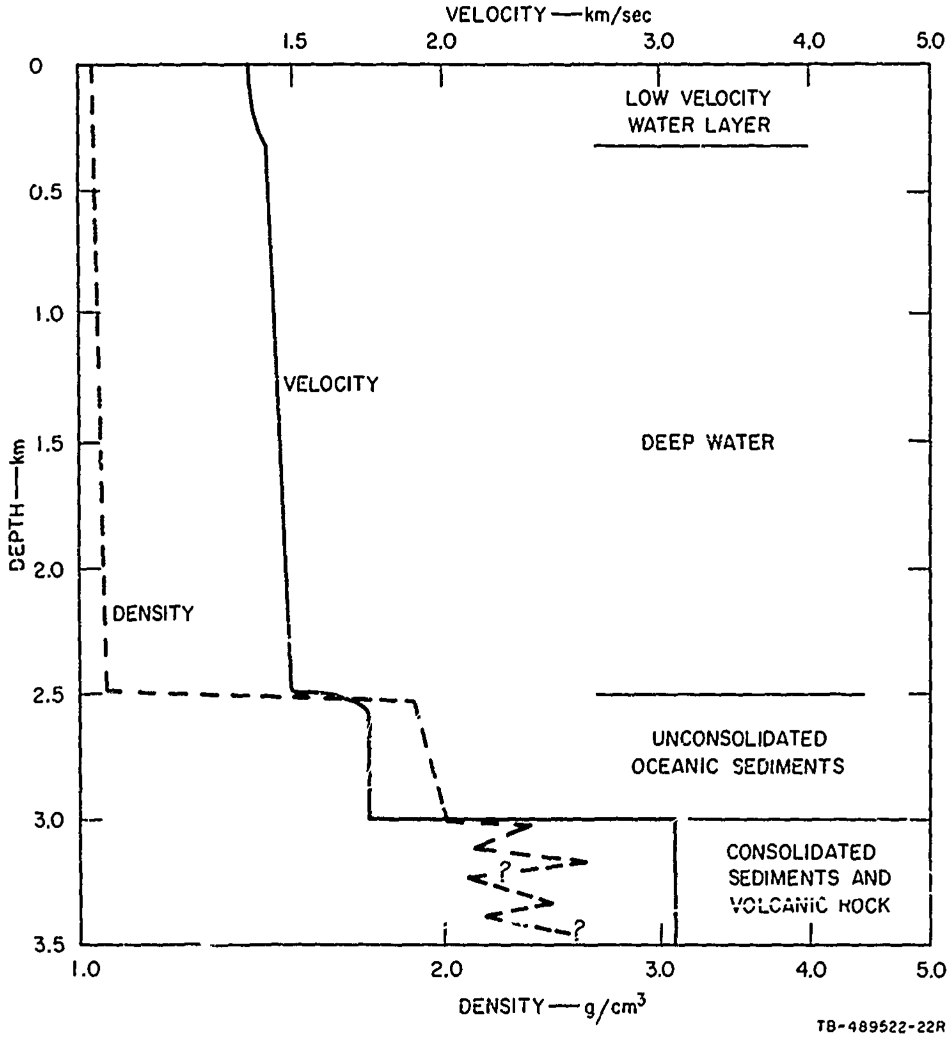

FIG. 3 VELOCITY AND DENSITY VARIATION IN THE CENTRAL ARCTIC OCEAN

In the shallow-water regions of the Arctic the acoustic velocity of the ice-covered waters probably increases slightly with depth as in the case of the deep waters. However, along the continental shelf the bottom itself causes a pronounced velocity increase at shallow depth.

In both environments there is a low-velocity channel near the water surface which results in guided wave propagation of acoustical disturbances. A portion of the energy emitted by a sound source is trapped in the low-velocity channel by a process of internal reflections. A downgoing disturbance in particle velocity will be reflected upward at some depth. At reflection, the wave will change phase, and if reflection is incomplete, a loss in amplitude will also occur. A similar occurrence will be experienced by an upgoing disturbance impinging on the ice. If the ice thickness is small compared to the wavelengths of sound in ice, then the ice has little effect on the reflection coefficient of the incident wave. That is, we may treat the water surface as a "free" surface and thereby assume complete reflection and a 180-degree phase change of the incident wave. This assumption was shown to be valid for ice less than 3 meters thick reflecting frequencies below 100 Hz (Goldstein, 1966).

To be precise, two waveguides exist: the near-surface water channel and the ice guide. At frequencies less than 100 Hz the phase velocities of free (trapped) vibrations of the ice are either smaller (flexual vibrations) or greater (longitudinal vibrations) than the phase velocities of the guided waves in the water (Press and Ewing, 1951). Therefore, there is no coupling of energy between the water and the ice layer, and our previous remarks that the ice can be ignored in the propagation of underwater sound still holds. However, for frequencies above 100 Hz we eventually must account for energy refracted into the ice. Depending on the ice thickness and angle of incidence, the refracted energy will be reradiated in varying degrees into the water or trapped within the ice layer. However, because of absorption and the irregular ice surfaces the ice layer waveguide is extremely lossy for high frequency propagation. We can, therefore, ignore the ice waveguide at source ranges of one kilometer and more.

In this report we shall address ourselves to the propagation of acoustic waves at or below 100 Hz. Although we recognize that the power radiated by

a submarine extends to frequencies well above 100 Hz we impose this frequency constraint because natural ice-vibration (noise) measurements are reported only at frequencies below 100 Hz, and because most of the submarine radiated power is also below 100 Hz. With this constraint, then, we outline below the basic theory and equations for guided wave propagation as they apply to deep (2.8 km) and shallow (0.1 km) ice-covered waters. In later sections we will consider, semi-quantitatively, the use of on-ice sensors at frequencies above 100 Hz.

For waves of constant frequency there will be only a finite number of ray directions that lead to the propagation of a large amplitude disturbance. The necessary condition for such a path is that constructive phase interference occurs at all points between the upward and downward reflecting interfaces. Clay (1964) describes this condition in terms of a phase integral

$$\int_0^h k(\vec{n}_m \cdot \vec{z})\,dz = m\pi \qquad (2)$$

where

- h = the vertical distance between reflecting surfaces
- k = the wave number = ω/α
- α = the compressional wave velocity in the layer, assumed here to be constant
- $\vec{n}_m$ = a unit vector in the direction of wave propagation that leads to constructive interference
- $\vec{z}$ = a unit vector in the vertical direction
- m = an integer, the mode number

and

$$k(\vec{n}_m \cdot \vec{z}) \equiv k_{mz}$$

Equation 2 carries no distinction between wave directions that lead to complete internal reflections and those that do not. We assume complete reflection at the surface for all angles of incidence; but at the lower

reflecting interface there will be a critical angle of incidence below which a portion of the energy will be refracted away with each reflection. At long ranges from the source the contribution from energy propagating at angles less than critical will be small. Therefore, we will include in our analysis only the contribution of those waves unattenuated by bottom refractions. With this constraint there exists for each mode, m, a low frequency cut-off corresponding to critical angle reflection (Officer, 1958).

Acoustic waves satisfying Eq. 2 will be dispersive, i.e., different frequencies will travel with different phase and group velocities and, depending on the number of solutions (modes) permissible, a particular frequency can have several different phase and group velocities. This dispersion is caused by the variation of velocity with water depth and is referred to as geometrical dispersion (Officer, 1958).

The phase integral condition is the basis for the theory of normal mode propagation. This approach to the evaluation of disturbance intensities propagating in a waveguide is particularly useful because of the analytical solutions developed by Pekeris (1948) and Tolstoy (1955, 1958), among others. With these solutions we have been able to evaluate the surface particle velocity amplitudes from a point source within models of the Arctic Ocean and shallow-water Arctic areas. These amplitudes have been calculated at ranges for which the normal mode approach is applicable, at horizontal ranges greater than several layer thickness. In this section a brief exposition of the analytical approach will be given. Additional material concerning the analysis is found in Appendix A.

At distances from the source for which unattenuated normal mode propagation is applicable, the particle velocity signal at frequency ω will be a superposition of signals from M modes. Assuming a simple harmonic point source the vertical and radial components of particle velocity can be expressed as:

$$V_z(R,Z,t) = -\sum_{m=1}^{m=M} [k_{mz} \cot (k_{mz}Z) D_m(k_{mr}R) F_m(k_{mz}Z, k_{mz}Z') \exp (i\omega t)] \qquad (3a)$$

$$V_r(R,Z,t) = -\sum_{m=1}^{m=M} \{D_m(k_{mr}R)F_m(k_{mz}Z,k_{mz}Z')\}(4R)^{-\frac{1}{2}} + ik_{mr}\} \exp(i\omega t)] \qquad (3b)$$

where

V_z = the vertical component of particle velocity

V_r = the horizontal component of particle velocity

R = the horizontal range from source to receiver

Z = the depth of receiver

Z' = the depth of source

k_{mr} = the eigen wave number

and

$$k^2 = k_{mz}^2 + k_{mr}^2$$
$$i = \sqrt{-1}$$

The value M will be finite but will increase with increasing ω. As we see from Eq. 3a and 3b the expressions for particle velocity are composed of two terms D_m and F_m that have only radial and vertical arguments, respectively. At large values of R the radial function can be approximated by:

$$D_m(k_{mr}R) = R^{-\frac{1}{2}} \exp[-i(k_{mr}R + \pi/4)] \qquad (4)$$

which shows that these waves spread cylindrically (as $R^{-\frac{1}{2}}$ instead of R^{-1}) and that the modes are displaced in phase from each other by an amount that depends on the range and the waveguide eigen values, k_{mr}. In an environment for which guided waves may exist the cylindrical spreading of energy permits the long range propagation of sound. The phase displacement between modes is a consequence of the dispersive nature of guided wave propagation.

Near the surface, or within the low-velocity near-surface channel, the function F_m can be expressed as:

$$F_m(k_{mz}Z, k_m Z') = W_m(k_{mz}h) \sin (k_{mz}Z) \sin (k_{mz}Z') \qquad (5)$$

The sinusoidal depth dependencies of this function are due to the standing wave nature of the guided modes. F_m is a maximum whenever source and receiver are at antinodes and a minimum at nodes of the standing wave pattern dictated by the values of k_{mz} that satisfy Eq. 2. The waves, of course, are not standing waves as may be excited in an organ pipe; they are traveling waves. From Eqs. 3a, 3b, and 5, it can be seen that the vertical particle velocity will be a maximum and the radial particle velocity will be zero at the surface for a source at any depth in the near-surface low-velocity channel. This is a consequence of the free-surface boundary condition which, for a thin ice cover, is a valid assumption at frequencies below 100 Hz. Because V_r is zero at the surface we shall ignore the radial component of velocity in subsequent discussions.

The function W_m $(k_{mz}h)$ in Eq. 5 is the excitation function for the m-th mode. It is a measure of the power radiated into the mode and depends on the source power output, the frequency of excitation, and the physical parameters of the medium. A simplified approach to the evaluation of the eigen wave numbers and Wm $(k_{mz}h)$ is first to approximate the inhomogeneous acoustical environment by N horizontal layers, each with a constant velocity and density. By means of this approximation Tolstoy (1955) describes how W_m may be numerically evaluated for an arbitrary system of N layers (Appendix A). Pekeris (1948) gives an exact algebraic expression for W_m for the two- and three-layer cases, and Pekeris' solution was used in the calculations presented here. In the two-layer case, only one lower reflecting interface at a depth h beneath the surface, the function W_m is:

$$W_m(k_{mz}h) = \frac{2}{\omega}\left(\frac{\alpha_1 P}{k_{mr}\rho_1}\right)^{1/2} k_{mz}L_m^{-1} \qquad (6)$$

where

$$L_m = k_{mz}h - \sin (k_{mz}h) \cos (k_{mz}h) - [\rho_1 \sin (k_{mz}h)/\rho_2]^2 \tan (k_{mz}h)$$

The ω^{-1} factor occurs because we have purposely chosen to represent the source by one whose power output is constant at all frequencies in an infinite, homogeneous medium*. This was done so that the computed particle velocity intensities at various frequencies could be directly compared for unit power output.

Because our objective is to obtain a measure of V_z at the surface (Z=0) caused by the superposition of all possible modes, we ignore the $e^{i\omega t}$ term in Eq. 3a and solve for the modulus of this complex expression:

$$|V_z(R,0)| = (V_z \cdot \bar{V}_z)^{1/2}$$

where $\bar{V}_z$ is the complex conjugate of V_z. This multiplication yields the following representation for the particle velocity;

$$|V_z(R,0| = \frac{2}{\omega}\left(\frac{\alpha_1 P}{\rho_1 R}\right)^{1/2} \left\{ \sum_{m=1}^{m=M} (k_{mz}^2 \sin (k_{mz}Z')/k_{mr}L_m)^2 \right.$$

$$+ 2 \sum_{n=1}^{n=M} \{k_{mz}^2 k_{nz}^2 \sin (k_{mz}Z') \sin (k_{nz}Z') \cos [R(k_{mr} - k_{nr})]$$

$$\left. \times (k_{mr}k_{nr}L_m L_n)^{-1} \right\} \qquad (7)$$

Equation 7 shows that the amplitude $|V_z (R,0)|$ is the sum of two terms both of which attenuate as $R^{-1/2}$: a constant term and a fluctuating term caused by the phase interference of the various modes. This equation forms the basis for the data to be presented. However, before discusing the numerical results it is important to consider some of the restrictions on the accuracy of the numerical evaluations.

In general, the amplitude fall-off that might be observed experimentally is greater than $R^{-1/2}$ for several reasons. For a shallow water environment,

*A velocity potential source with the form $(A/\omega)\exp i\omega t$ will yield the desired effect (Tolstoy, 1958).

attenuation of the guided waves can be caused by the sloping of the bottom, incomplete reflection due to shear waves refracted into the bottom, roughness of the bottom and under-ice surfaces, and the porous nature of bottom sediments. We can safely ignore thermoelastic effects and volume scattering for low-frequency waves. For a deep water environment, potential causes for attenuation are lateral variations in acoustic impedance and roughness of the ice bottom.

To account for the effects of attenuation other than spreading losses, investigators have taken several approaches. For example, to better describe wave propagation in shallow water where bottom losses occur the eigen wavenumbers can be made complex, $\varkappa_{mr}=k_{mr}+ i \epsilon_{mr}$. Provided the values ϵ_{mr} are small, and experiment seems to confirm this (Ewing, Pekeris, and Worzel, 1948; Tolstoy, 1958), the eigen values, k_{mr}, are not perturbed by the addition of the imaginary component and Eq. 3 is modified only to the extent that D_m takes on an $\exp(-\epsilon_{mr}R)$ factor.

Brekhovsikikh (1960) analyzed the condition of imperfect reflections at one of the boundaries and showed that for large ranges (large compared to the waveguide thickness) the average decay of signal intensity could be represented by a $R^{-3/4}$ fall-off. This fall-off is intermediate between the cylindrical law ($R^{-1/2}$, perfect reflection) and the spherical law (R^{-1}, no reflection).

Clay (1964) extended Eckart's (1953) study of the reflection of plane waves from slightly irregular surfaces and was able to show the effect of an irregular reflecting interface on guided wave propagation. When such a surface exists a portion of the guided wave energy may be scattered in a direction that does not satisfy the phase integral (Eq. 2). The rate of attenuation increases with height of the surface irregularities, acoustic wave frequency, and mode number.

In the following presentations of calculated signal (particle velocity) amplitudes we include the ice roughness attenuation on the guided waves. The development for the correction term that must be incorporated into Eq. 7 is given in Appendix B. Here we will explain only that for the attenuation we assume the ice bottom to be a random surface with a Gaussian distribution of amplitudes. The standard correction factor employed throughout is based on a 3-meter standard deviation in the surface irregularities, a value proposed

by Mellen and Marsh (1965) from their experiments in measuring the scattering of sound by Arctic sea ice.

Comparison of Signal and Noise Amplitudes on the Surface of an Idealized Arctic Ocean

The Arctic Ocean acoustical environment of Fig. 3 was partitioned into three homogeneous layers with properties shown in Table 1.

Table 1

The Approximation for the Deep Water Environment

Layer	Velocity (m/sec)	Density (gm/cm^3)	Thickness (m)
1	1441	1.028	350
2	1480	1.039	2450
3	1525	1.400	∞

The surface layer was given a velocity and density corresponding to the average values found in the region of the near-surface segment of the roughly bilinear, oceanic velocity variation (Fig. 3). To the middle layer we assigned a velocity and density equal to the average values of the lower segment of the bilinear velocity variation. The bottom layer, or half-space, was given the approximate acoustical properties of water-saturated oceanic sediments. It turns out that the magnitude of velocity and density assigned the ocean-bottom rocks has a negligible influence on the normal mode propagation because this region does not reflect the guided waves. That is, as we have formulated the problem, the lower reflecting surface of the waves is the interface between layers 1 and 2. This is a simplification of the true conditions but is judged adequate for the objective of this study.

Shown in Fig. 4 are the phase velocity dispersions for the first 11 modes calculated for the simplified acoustical representation of the Arctic Ocean. The eigen wave numbers k_{mr} are related to the phase velocities by the relation $k_{mr} = \omega/c_m$. As an intermediate step toward the numerical evaluation of the particle velocity intensities at the surface of the water, the

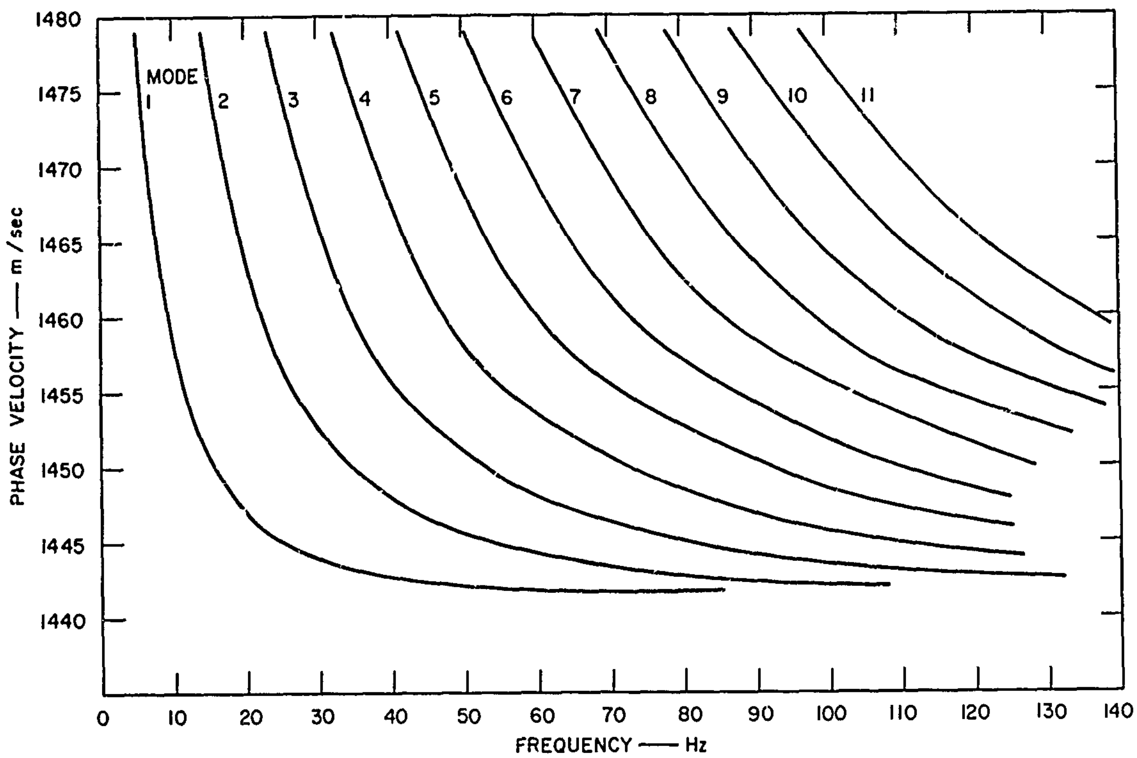

FIG. 4 CALCULATED PHASE VELOCITY DISPERSION OF GUIDED WAVES IN DEEP ARCTIC WATER

excitation, a measure of the signal strength of each mode, was calculated using the eigen wave number information (see, for example, Eq. 3a, 6). These excitation strengths, shown in Fig. 5, represent a mode-by-mode numerical evaluation of Eq. 3a for a source emitting a constant one-watt acoustical power at all frequencies. In this representation we ignore the time dependency and set D_m equal to unity to eliminate the effect of range and and phase. The choice of one-watt in the calculations is made with the realization that one watt is probably more power than found in individual lines of a submarine line spectrum. However, unit power output is used here and throughout all subsequent discussions, and the numerical results presented may be adjusted to any desired output power merely by multiplying by the square root of that power in watts (Eq. 6).

The excitation strengths illustrate the transparency of the Arctic Ocean environment for guided wave propagation with respect to mode number, frequency,

and source depth.. For example, Fig. 5 shows how changing source depth affects the excitation of 10 Hz normal-mode vibrations. As the source depth increases from 25 to 125 meters the resulting signal amplitude will increase by a factor of almost five.

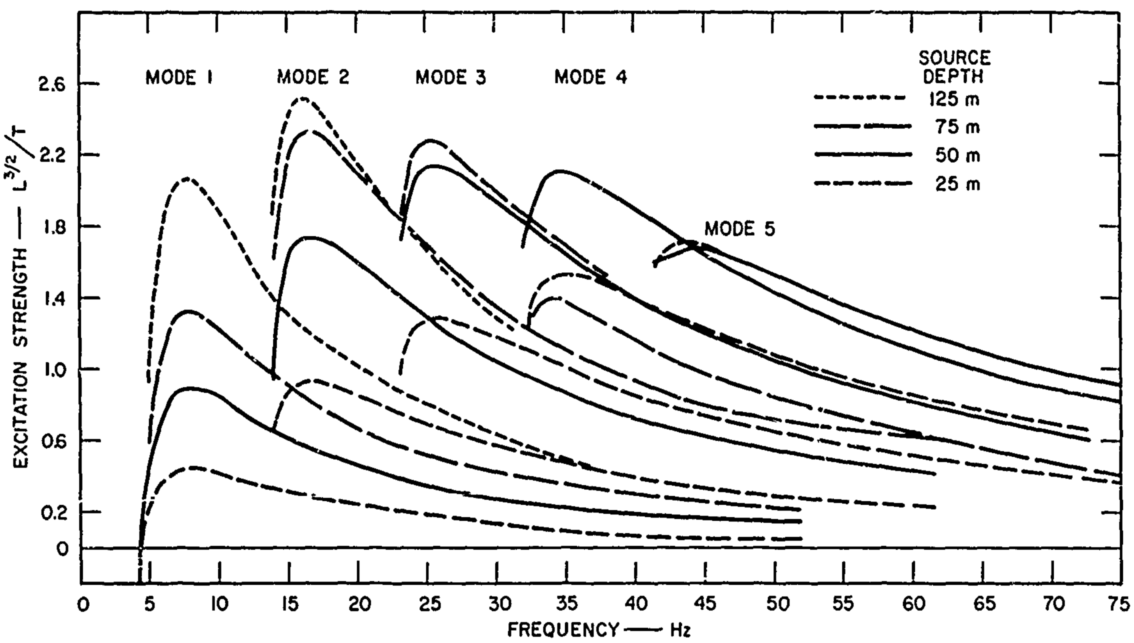

FIG. 5 CALCULATED RELATIVE EXCITATION STRENGTHS OF A FEW MODES FOR VARIOUS SOURCE DEPTHS IN DEEP ARCTIC WATER

Of more specific interest than the curves in Fig. 5 are the range-dependent amplitudes $|V_Z|$ for particular frequencies calculated according to Eq. 7. Shown in Fig. 6 are the results of these calculations for a 25-Hz source at depths of 25, 50, 75, and 125 meters. At this low frequency only three modes contribute to the total signal amplitude, and comparative calculations showed that ice-bottom roughness had negligible effect on signal amplitudes out to the maximum range considered. Included in Fig. 6 for comparison are the signal amplitudes calculated for the case where the top layer becomes infinitely thick: Curves A, B, and C.

To illustrate the relative magnitude of the calculated signal amplitudes

and the observed ambient noise amplitudes, the maximum and minimum noise levels at 25 Hz are indicated in Fig. 6. These data were taken directly from the curves in Fig. 2. Also included in Fig. 6 is a decibel scale which gives the signal amplitude in terms of dB's above the minimum noise level observed. A general conclusion is that because the signal amplitude from the assumed 1-watt source lies close to the minimum natural noise level there will be periods when the background noise will completely overwhelm the signal.

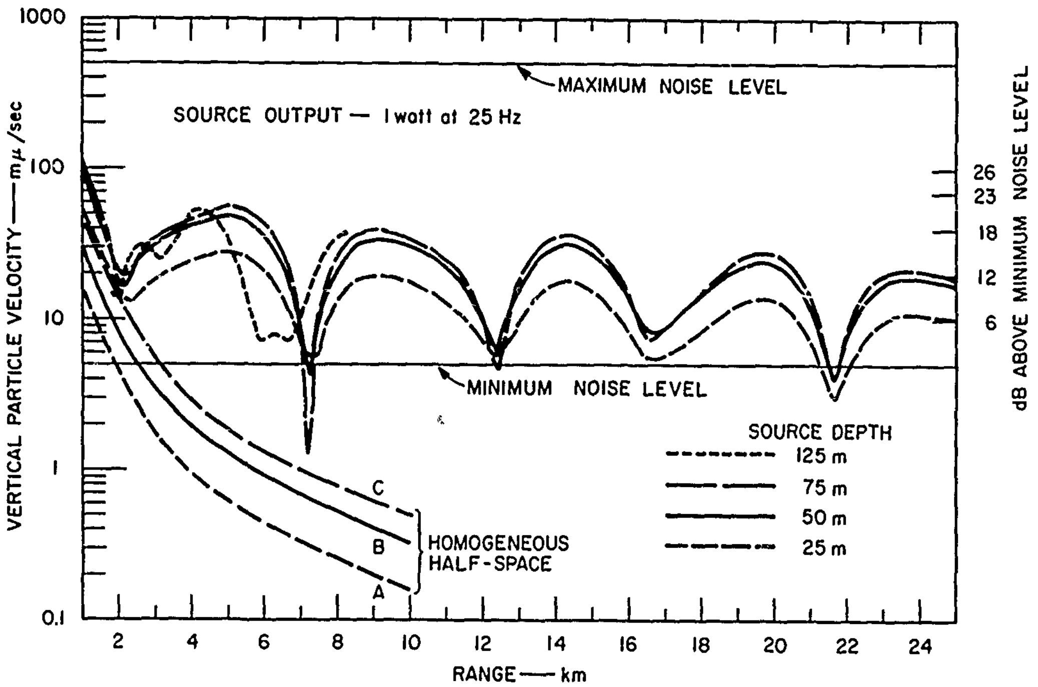

FIG. 6 VERTICAL PARTICLE VELOCITY AS A FUNCTION OF RANGE FOR VARIOUS SOURCE DEPTHS (Three Modes, 25 Hz)

To develop a less general conclusion we would need to know the most likely noise amplitude occurring at a given time of day and season of year. Existing data is insufficient to permit a complete analysis, but Prentiss' data have been used to plot observed noise amplitudes versus local time, observed from 26 April through 14 May 1962 (Fig. 7). The data suggest no correlation between noise intensity and time of day. However, the data at any instant were well above the minimum level. As an arbitrary dividing point,

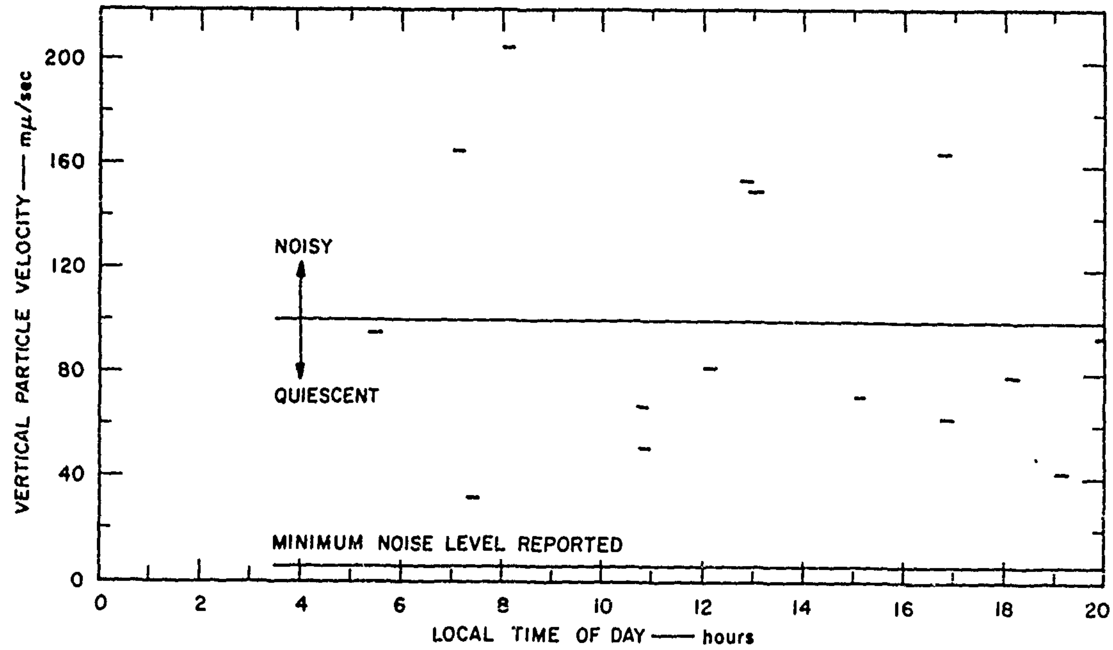

FIG. 7 AVERAGED VERTICAL PARTICLE VELOCITIES OF 25-Hz NATURAL ICE VIBRATION, 26 APRIL TO 14 MAY, (After Prentiss et al, 1965)

100 mμ/sec was chosen as the separation between noisy and quiet conditions. Considering just the amplitudes during the "quiet" intervals we find that average noise is approximately 65 mμ/sec; a noise amplitude that is uniformaly greater than the calculated amplitudes signal except at very short ranges from the source. Thus, even under essentially quiet conditions a source output of at least 4 watts would be required to detect a source within 20 km.

The unfavorable signal-to-noise relation worsens when we consider frequencies of 50 and 100 Hz. For 50-Hz propagation the signal amplitudes corresponding to several source depths are plotted against range in Fig. 8. In Fig. 9 it may be seen how the ice-roughness attenuation alters the numerical value for $|V_z|$: scattering of 50-Hz acoustic waves by the ice bottom leads to slightly smaller signal amplitudes.

For 100-Hz propagation, the effect of ice roughness is more inhibiting to the signal amplitudes. Figures 10 and 11 show that the ice bottom roughness causes a noticeable attenuation beginning at a range of about 10 km.

Beyond a range of 20 km the attenuation amounts to 6 dB or more in places.

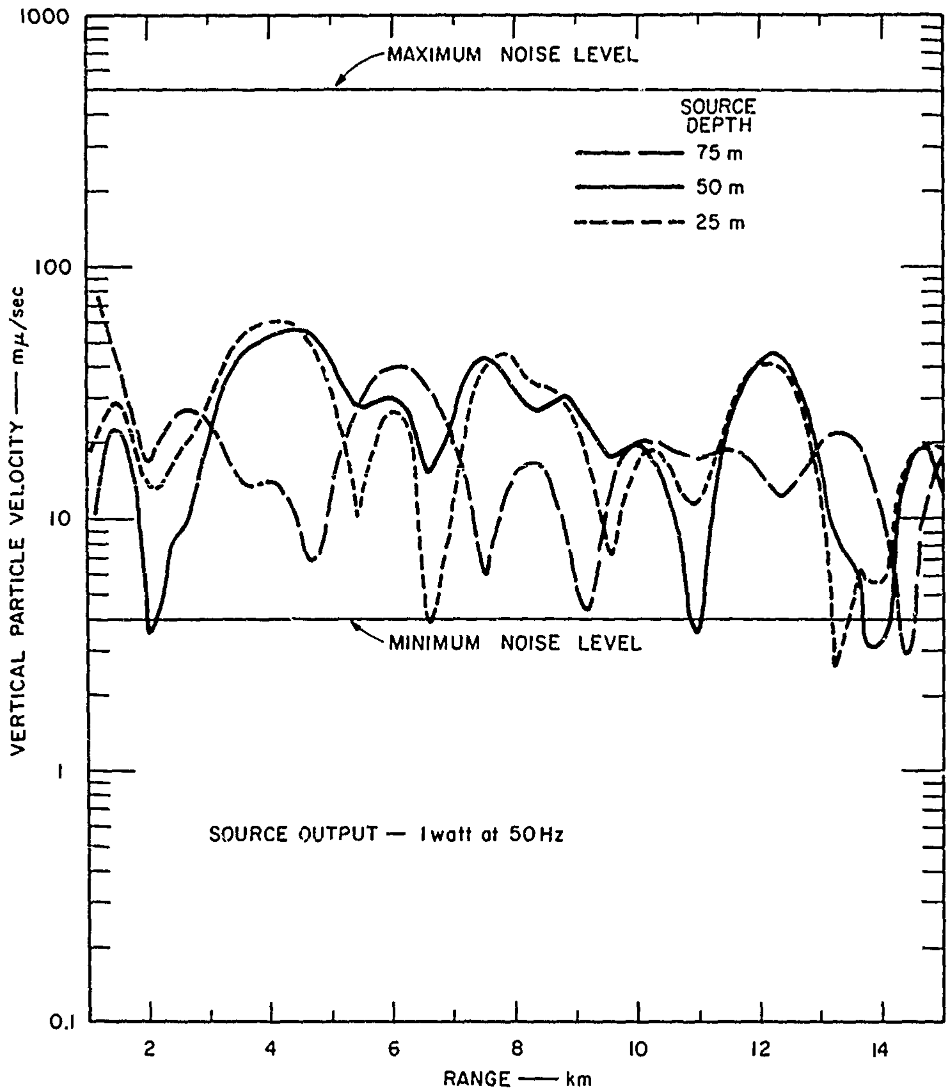

FIG. 8 VERTICAL PARTICLE VELOCITY AS A FUNCTION OF RANGE FOR VARIOUS SOURCE DEPTHS (Six Modes, 50 Hz, Ice Bottom Irregularities Ignored)

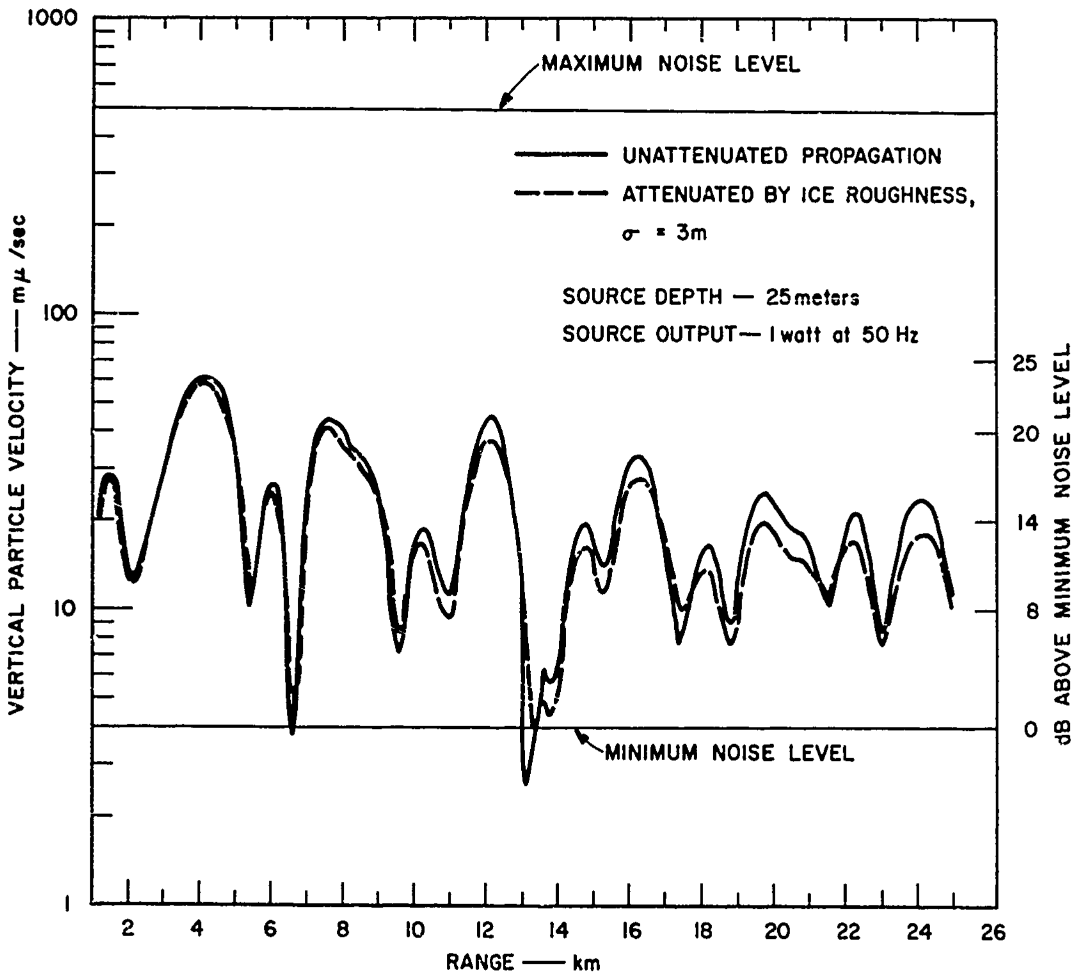

FIG. 9 VERTICAL PARTICLE VELOCITY AS A FUNCTION OF RANGE: 50-Hz OUTPUT, SOURCE DEPTH 25 METERS (6 Modes)

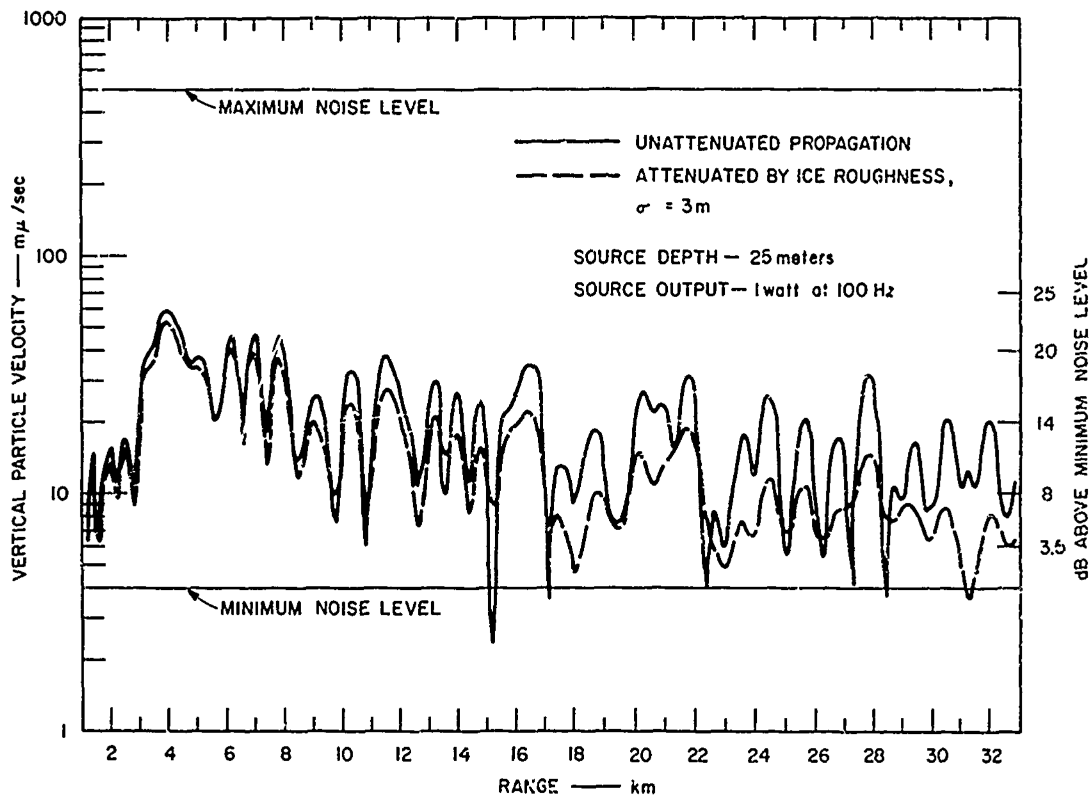

FIG. 10 VERTICAL PARTICLE VELOCITY AS A FUNCTION OF RANGE: 100-Hz OUTPUT, SOURCE DEPTH 25 METERS (11 Modes)

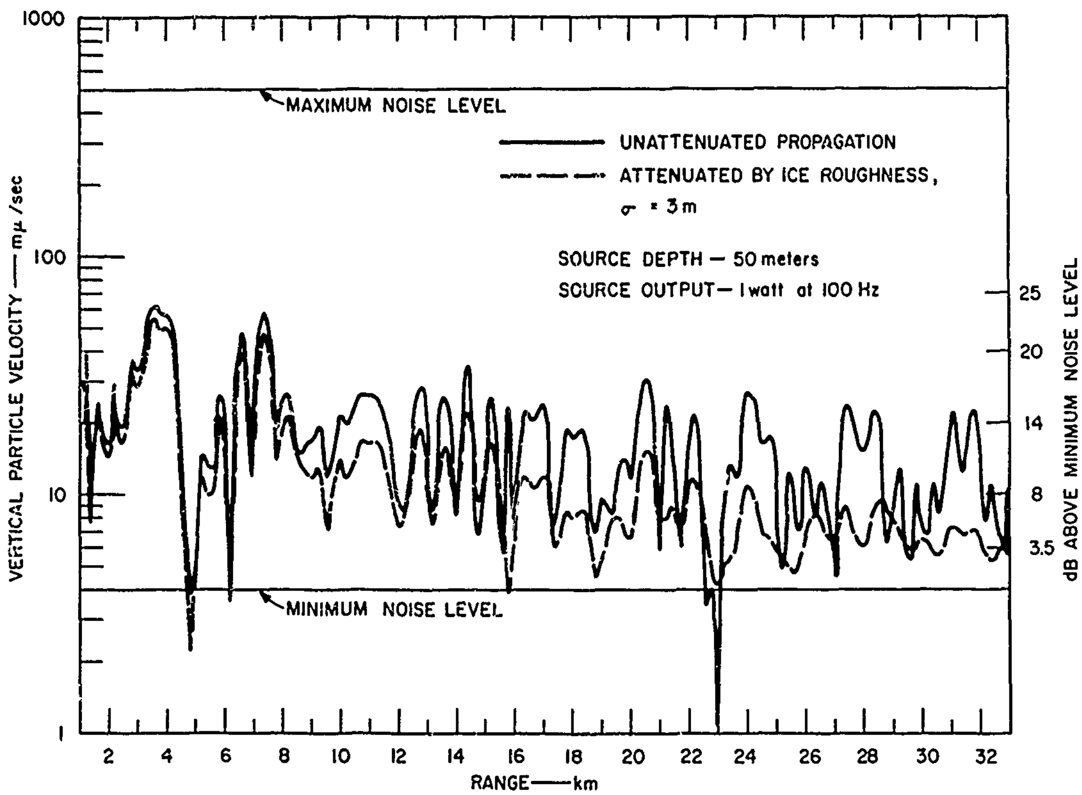

FIG. 11 VERTICAL PARTICLE VELOCITY AS A FUNCTION OF RANGE: 100-Hz OUTPUT, SOURCE DEPTH 50 METERS (11 Modes)

At both 50 and 100 Hz the signal intensities remain, in general, above the observed minimum noise level out to the maximum ranges considered, but the signal intensities are so close to the minimum noise level that unless a condition of extreme quiet exists the weak signal would not be perceptible above the ambient noise. Again using the information given by Prentiss et al (1965) we find the average noise was 235 mμ/sec at 50 Hz for six recording sessions between 18 and 27 April 1962. During the same time interval the average noise was 257 mμ/sec at 100 Hz, based on only four recording sessions. Although the data are too few to yield a reliable estimate, the average noise given suggest that unless the source emits far more power than 1 watt at 100 Hz its detection will be hampered by the presence of ambient noise.

The best signal-to-noise ratio exists at relatively low frequencies, 5 to 10 Hz. In Fig. 2 the maximum observed noise level is shown to drop sharply at 10 Hz, falling from about 200 mμ/sec at 10 Hz to 10 mμ/sec at 7 Hz. As guided wave propagation is strongly excited at 7 Hz (Fig. 5) it seems that an on-ice transducer should be most useful if the source sought emits strong spectral lines at 7 or 8 Hz. A source emitting a one-watt line at 7 Hz will yield a particle velocity signal at short ranges (< 30 km) that we estimate from the curves to be roughly equal to the maximum noise level.

Comparison of Signal and Noise Intensities on the Surface of an Idealized Shallow Water Arctic Region

There exists in the Arctic and Subarctic a large total area of relatively shallow water which has a seasonal cover of land-fast or pack ice. Because parts of these shallow coastal waters are deep enough to allow the operation of a fleet-class submarine, the use of geophones on their ice covers should be considered. In this section we present the calculated signal intensities for guided waves propagating within a generalized shallow water environment. This we have taken to be a homogeneous water layer 100 meters thick underlain by a homogeneous half-space. The characteristics of this model environment are shown in Table 2. Our presentation of the numerical results is the same as employed in the discussion of the Arctic Ocean environment.

Table 2

The Approximation for the Shallow Water Environment

Layer	Velocity (m/sec)	Density (g/cm^3)	Thickness (m)
1	1436	1.026	100
2	2000	2.00	∞

For the environmental parameters listed in Table 2 the phase velocity dispersion for various modes was calculated and is shown in Fig. 12. Based on this information the relative signal strengths in each of the first 10 modes was calculated for source depths of 25 and 50 meters, Figs. 13 and 14, respectively. These strengths were then combined with the range information in a manner described earlier to yield the variation of particle velocity amplitude with range at frequencies of 20, 50, and 100 Hz. We again assume unit power output at all frequencies.

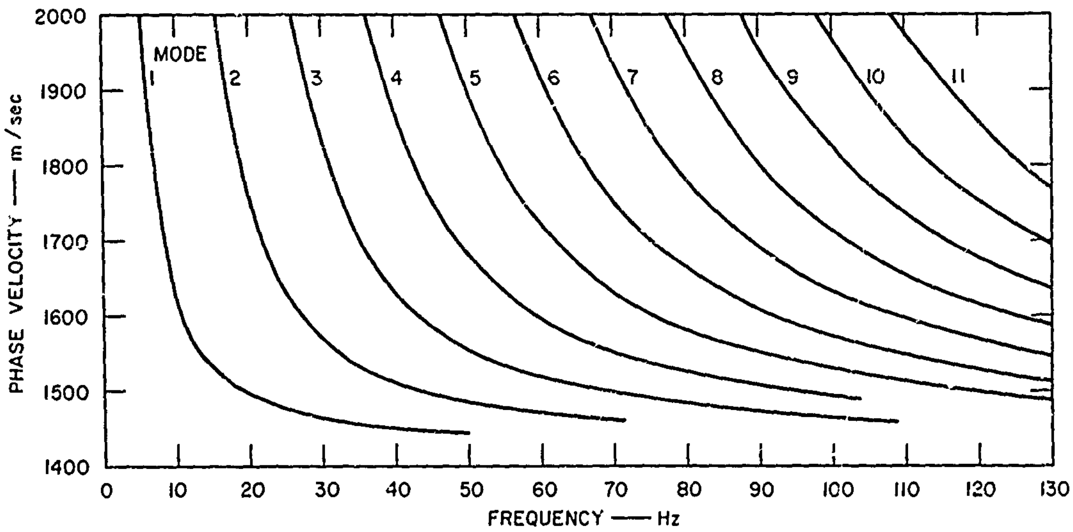

FIG. 12 CALCULATED PHASE VELOCITY DISPERSION OF GUIDED WAVES IN SHALLOW ARCTIC WATER

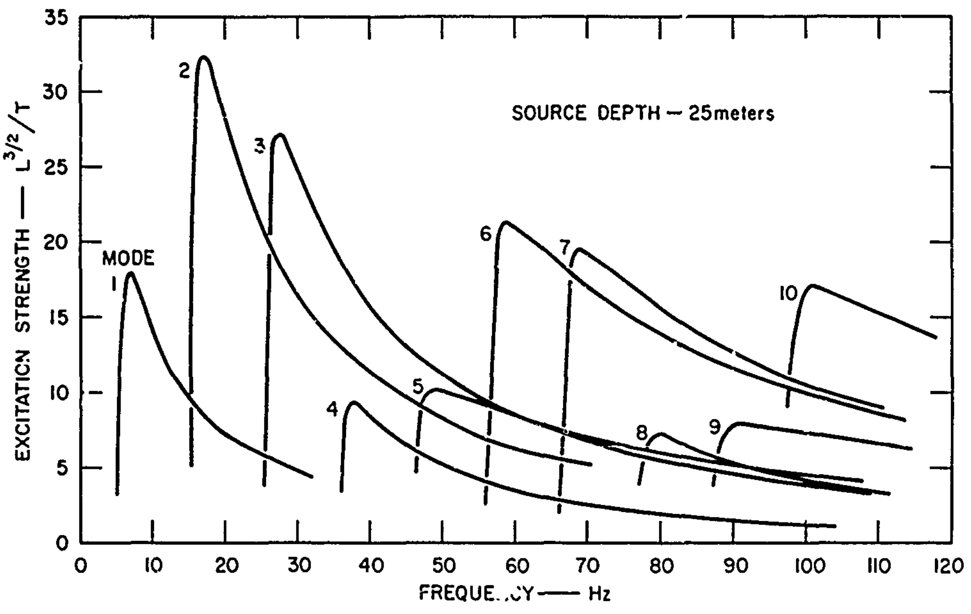

FIG. 13 EXCITATION STRENGTH OF FIRST 10 NORMAL MODES IN SHALLOW ARCTIC WATER, SOURCE DEPTH 25 METERS

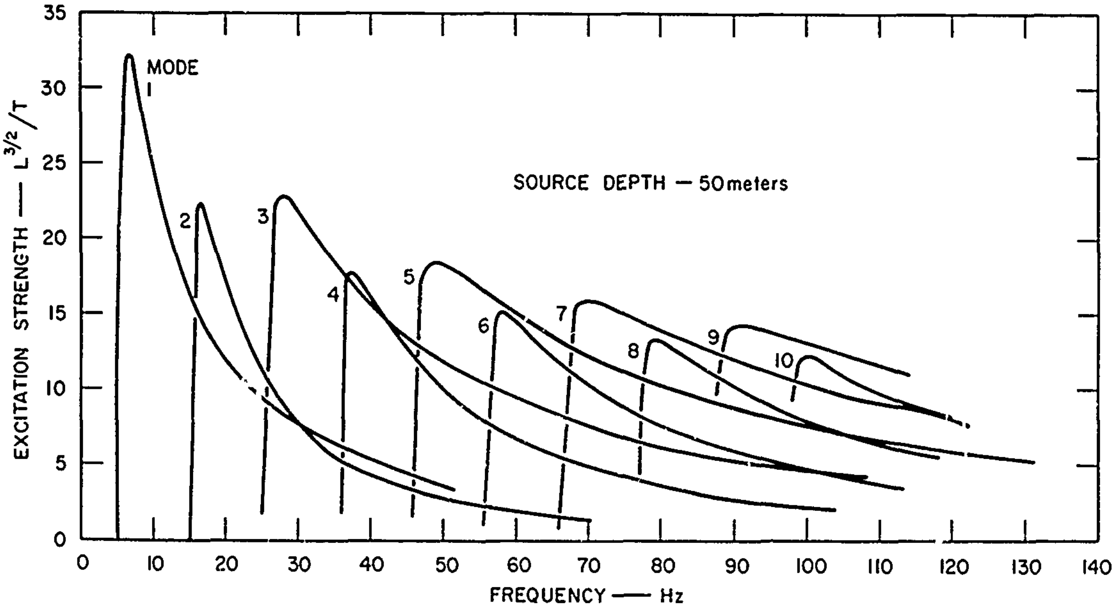

FIG. 14 EXCITATION STRENGTH OF FIRST 10 NORMAL MODES IN SHALLOW ARCTIC WATER, SOURCE DEPTH 50 METERS

For a 20-Hz source the amplitudes are plotted against range in Fig. 15. The uppermost curve (dashed) corresponds to the signal amplitudes from a source at a depth of 25 meters when the roughness of the ice bottom is ignored. However, in a shallow water environment the number of reflections per waveguide distance is larger than in a deep water environment, and the scattering of incident waves by the ice irregularities causes a significant attenuation, even for frequencies as low as 20 Hz. This may be seen in Fig. 15 by comparing the dashed curve to the solid curve for a source depth of 25 meters.

We do not know if we are justified in using for this environment the attenuation factor based on a 3-meter standard deviation in ice roughness. We rather suspect that this value, and thus the resulting attenuation, is too large in relation to the smaller ice thicknesses found in some ice-covered coastal regions. However, since we do not include the effects of other causes for attenuation in shallow water, such as shear wave conversion and bottom irregularities, the correction factor probably does not yield unrealistic values of signal amplitude.

The ice-bottom roughness results in an unequal attenuation of the modes of propagation. This is indicated in Fig. 15 by the phase interaction between the first two modes, which is negligible beyond a range of 8 kilometers after we include the roughness attenuation. The overall rate of attenuation appears to be slightly greater for a 25-meter source depth than a 50-meter source depth; a feature thought to be caused by the disparity in mode excitation strengths with changing source depth.

To our knowledge there has been no experimental work to determine the range of noise amplitude on ice in a shallow water environment; in Fig. 15 we have included for illustration only the maximum and minimum noise level of deep sea Arctic ice at 20 Hz. If these noise levels apply equally to both acoustic environments, there will be a more favorable signal-to-noise ratio in the shallow-water case than at a comparable frequency in deep water. This would be the case if more of the noise vibrations at 20 Hz are generated locally in the ice and propagate principally through the ice layer. On the other hand, the assumption that the noise is propagated through the water from distant sources as normal mode vibrations would imply that the signal-

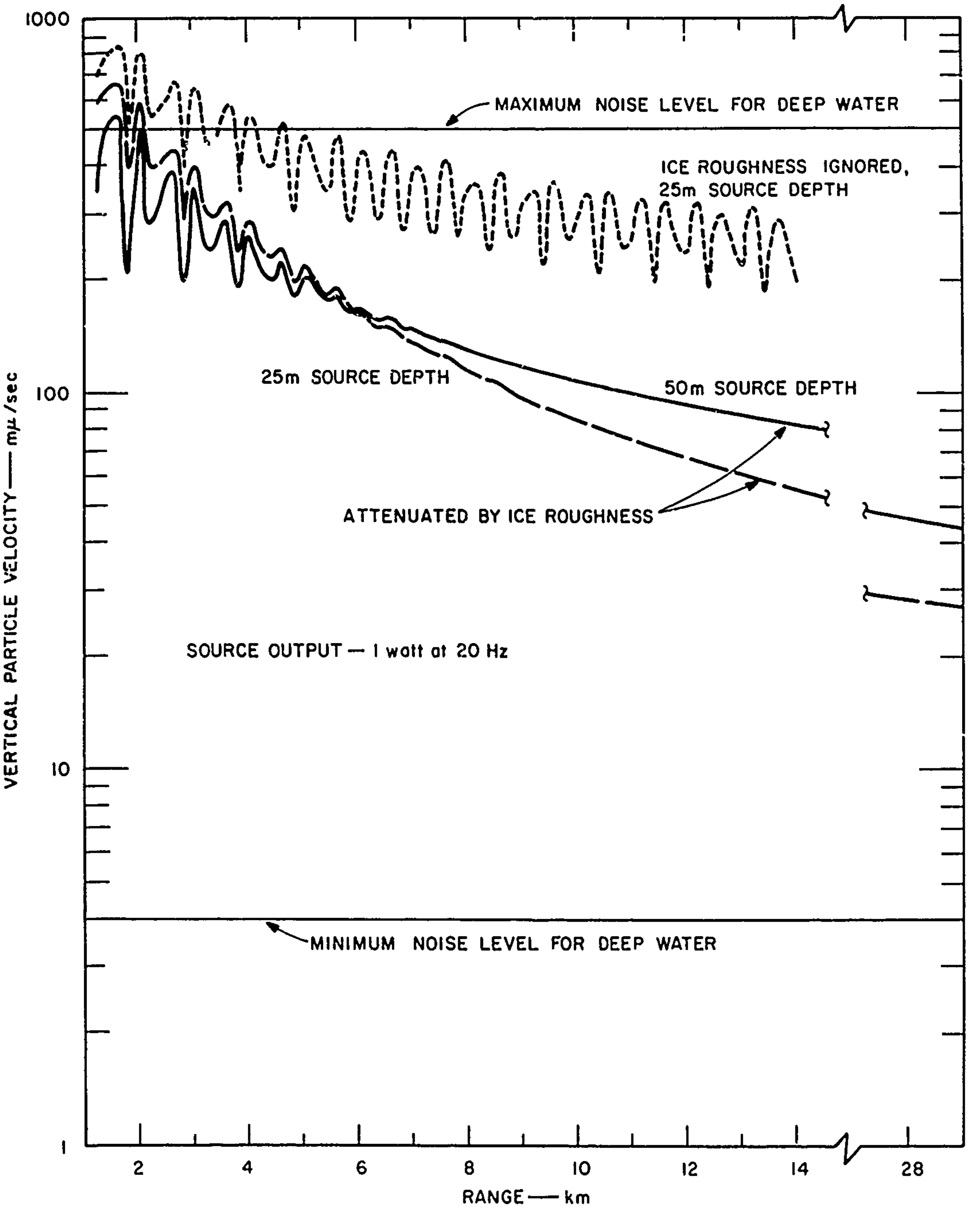

FIG. 15 VERTICAL PARTICLE VELOCITY AS A FUNCTION OF RANGE, SHALLOW ARCTIC WATER, 20-Hz OUTPUT

to-noise ratio in the shallow-water case could be as poor as in the deep-water case. That is, the shallow water environment, conducive to the strong excitation of normal mode vibrations, does not distinguish between the propagation of signal and noise disturbances. However, it is more likely that ice vibration noise is local and that a more favorable signal-to-noise ratio occurs in the shallow water case. Hence, despite the pronounced attenuation caused by ice roughness, the signal amplitude from a one-watt source could be equal to or greater than the likely noise amplitude* out to ranges of 14 kilometers.

Figures 16 and 17 show the calculated signal intensities at 50 and 100 Hz for sources 25 and 50 meters deep after the correction for ice-bottom scattering has been made. The scattering causes a rapid attenuation of signals at these higher frequencies. As a result the anticipated signal-to-noise ratios would be much less favorable than those in the 20-Hz case. A comparison between Figs. 11 and 17 reveals that the average signal level at 100 Hz is no better in shallow water than in deep water for sources of equal strength.

Comparison of Hydrophone and Geophone Signal-to-Noise Ratios

Comparisons have been made between signal-to-noise ratios for geophones and hydrophones equidistant from distant underwater explosive sources (Greene, Elbert, and Fitzpatrick; 1966). Relative signal-to-noise ratios are shown in Fig. 18, taken from Greene et al. The general conclusion from this work is that the hydrophone is a much better sensor, regardless of frequency and source range. This is perplexing at first glance. We would not expect the significant difference in the calculated ratios to occur because both pressure and particle velocity are analytically related to the same acoustic potential functions that describe signal and noise. Moreover, the relatively poorer ratios from the geophone data cannot be explained away by signal attenuation in the ice at the geophone site. The data given in the figure do not support this explanation.

*We assume here a likely noise amplitude of 65 $m\mu$/sec, a value explained in the previous section.

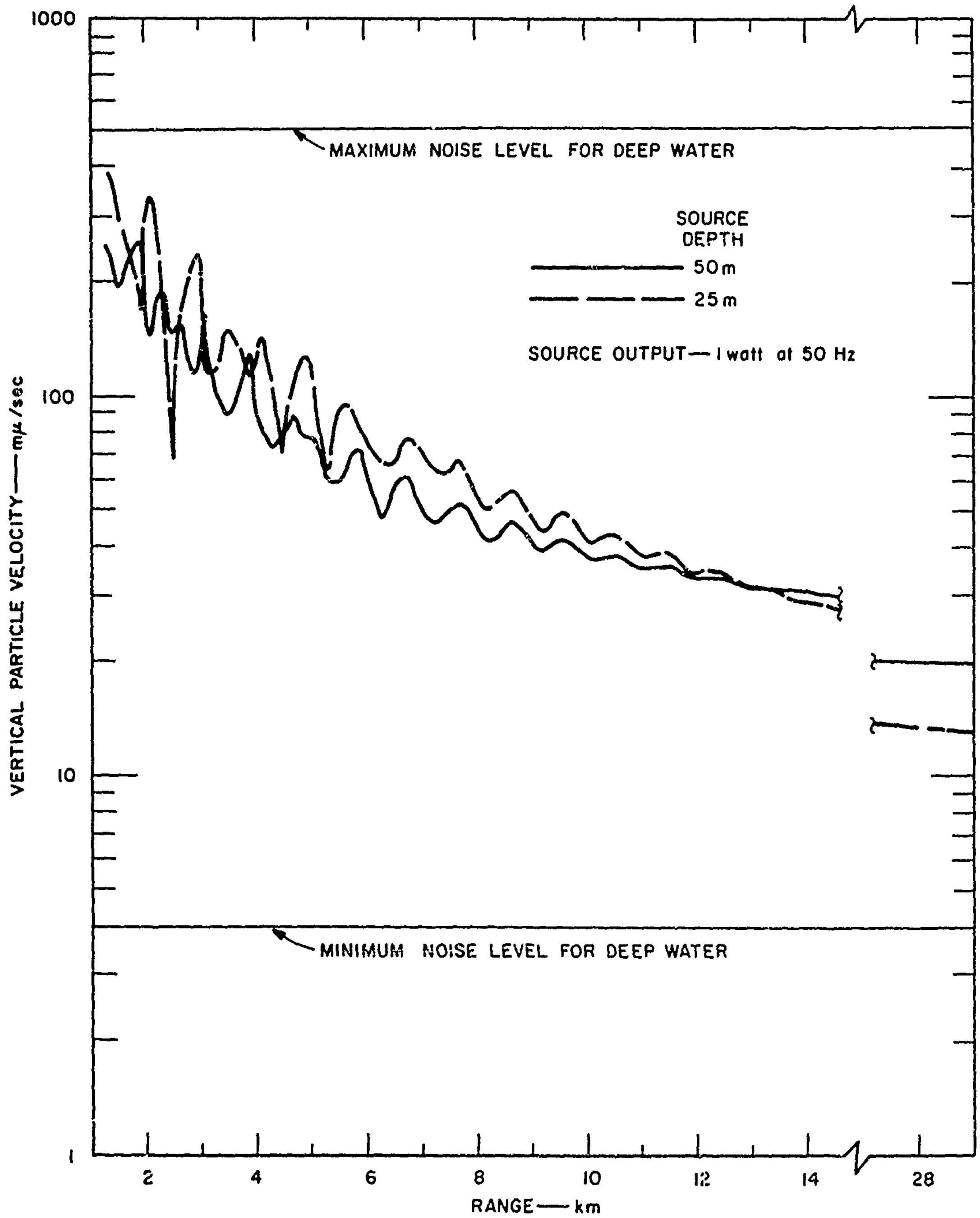

FIG. 16 VERTICAL PARTICLE VELOCITY AS A FUNCTION OF RANGE, SHALLOW ARCTIC WATER, 50-Hz OUTPUT

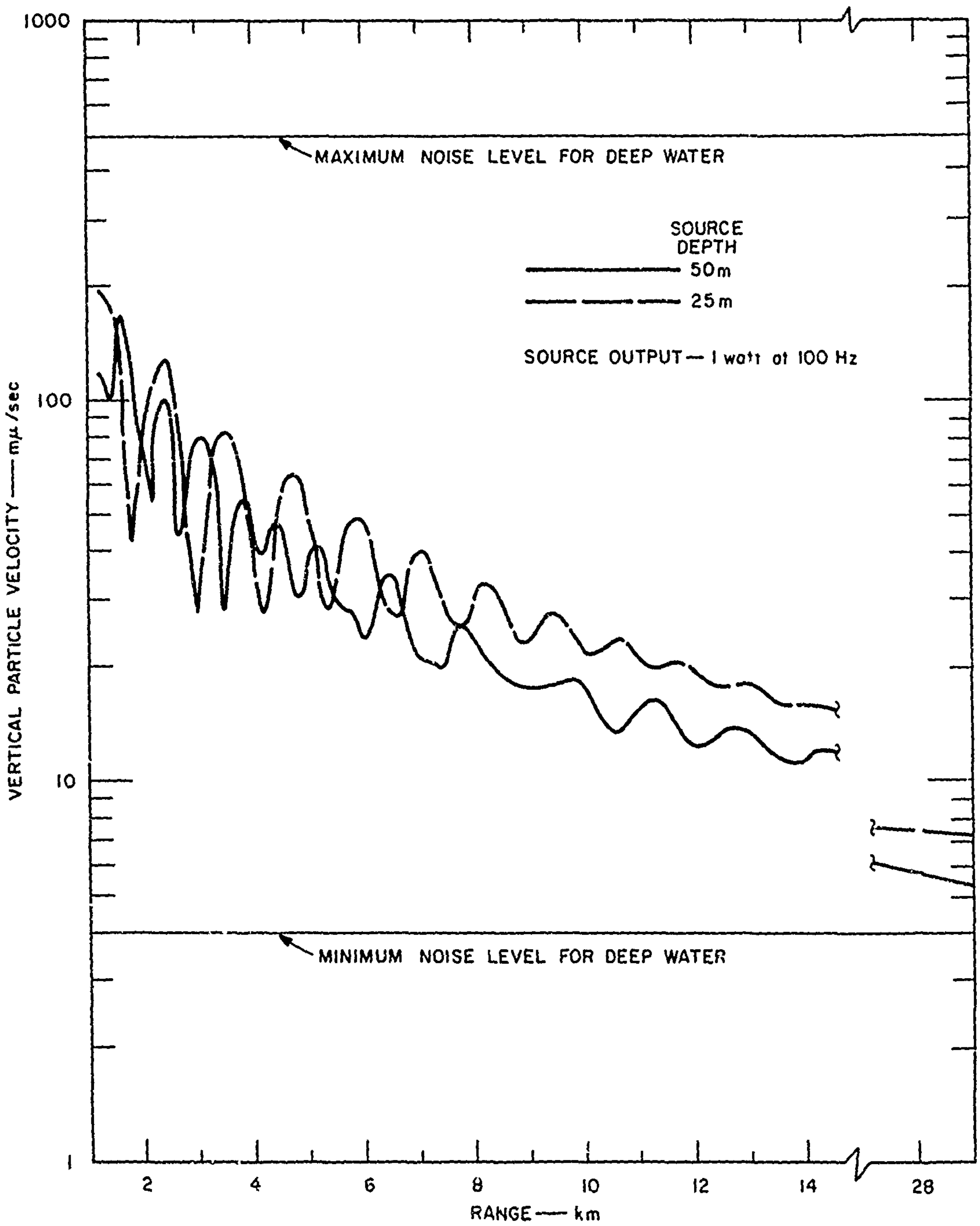

FIG. 17 VEPTICAL PARTICLE VELOCITY AS A FUNCTION OF RANGE, SHALLOW ARCTIC WATER, 100-Hz OUTPUT

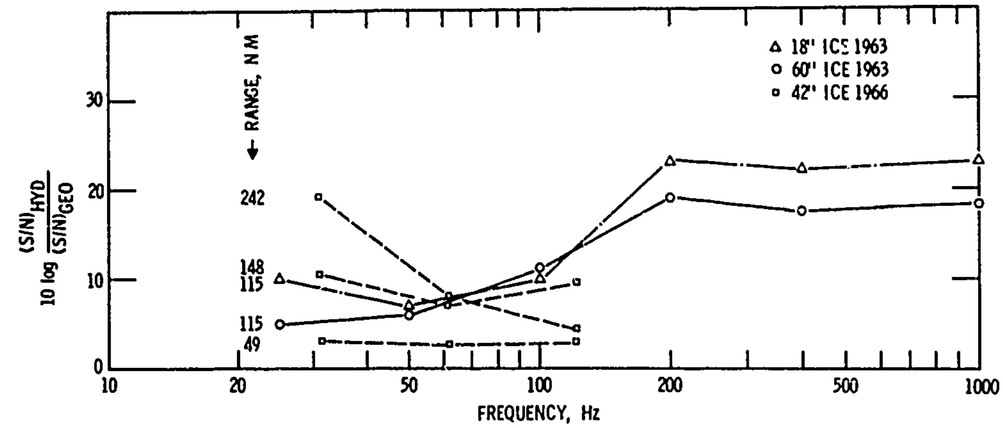

FIG. 18 COMPARISON OF HYDROPHONE TO GEOPHONE SIGNAL-TO-NOISE RATIO FOR SIGNALS RECEIVED FROM DISTANT EXPLOSIONS
(After Greene, Elbert, Fitzpatrick, 1966)

It is our belief that the ice is a relatively noisier environment than is the water at a depth of one hundred feet or so beneath the ice. This state could occur if seismic disturbances originating in the ice are effectively trapped within the ice layer, decaying exponentially in amplitude into the water. Various types of trapped waves are possible in a floating ice sheet (Press and Ewing, 1951); for example, the ice admits trapped longitudinal waves. This hypothesis does not explain the better relative geophone signal-to-noise from the nearest explosion reported (49 n.m.). Perhaps this was due to quiet ice conditions at the time of the experiment.

Over the 20 to 100-Hz bandwidth, specifically studied in this report, Fig. 18 shows that roughly a 20 dB better signal-to-noise ratio is obtained with a hydrophone. The data further indicate that above 100 Hz the hydrophone gives a 40 dB signal-to-noise improvement over the geophone. The marked difference above 100 Hz implies that noise sources in the ice must be extremely local (the ice strongly attenuates high-frequency vibrations). However, as we do not know the frequency response of the geophone nor the system noise, we cannot be sure that the 40 dB signal-to-noise difference is real at the higher frequencies where geophone sensitivity and the signal strength fall off.

Recognition and Localization of the Source

Recognizing and localizing a nearby underwater noise source in deep water with geophones is severely restricted by the natural ice vibrations, a fact brought out in the previous sections. Here we will not attempt to deal with recognition and localization in terms of acoustical outputs measured from submarines of various classes and traveling at different speeds. Our purpose is only to bring up a number of general points that have a bearing on the usefulness of geophones (and hydrophones as well).

The usual technique for improving signal-to-noise ratio is to deploy numerous sensors in arrays. Earthquake seismologists are well accustomed to the idea of giant arrays. The large-aperture seismic array (LASA) in Montana consists of over 500 seismometers in 21 clusters over a circular area of 200-km diameter. Recently, it was suggested (Press and Brace, 1966) that about 1000 seismometers be arrayed in selected locations of California and Nevada as part of an experiment to detect and locate earthquakes and micro-earthquakes. When the signal sought is coherent over a large area and the noise is not, array processing of seismometer outputs has led to an increase in the signal-to-noise ratio by a factor slightly greater than the square root of the number of sensors.

However, the two acoustic environments under discussion are dispersive, and this results in signals that are not, in general, spatially coherent.

The unhappy coincidence of unfavorable signal-to-noise ratio and dispersive signals does not, in theory, eliminate the possibility of localizing the source. However, a large number of on-ice transducers must be used for this purpose.

In a homogeneous medium the simplest means for localizing a source is a steerable array. The signals sensed by several colinear transducers are brought into phase by the introduction of various time delays. The necessary delays are related to the source azimuth.

In an inhomogeneous medium where guided wave propagation occurs, each frequency component will travel with a multiplicity of phase and group velocities, all of which will be different. In this situation time delay steering will not yield the true source azimuth. For example, Clay (1961)

studied array steering for the localization of a continuous signal source in a shallow-water waveguide, and showed that interference effects between modes led to a multiplicity of source azimuths. In this case three modes were dominant and three apparent source azimuths were indicated by the processed hydrophone output signals: one apparent azimuth was real but wrong and two apparent azimuths were imaginary. The source was colinear with the hydrophone array in Clay's study.

Only in the special case where the source azimuth is $\pm \pi/2$ radians with respect to the direction of the linear array may the source azimuth be correctly determined. In that case the traveling wave fronts are parallel to the line of detectors and the signals sensed are coherent. This suggests that if we were to deploy numerous linear arrays, each like a spoke radiating from the hub of a wheel, the linear element whose summed and squared signal is a maximum is most nearly parallel to the signal wave fronts.

The number of sensors necessary in each linear element is a subject of concern. The more sensors used the greater the signal enhancement and the less chance of correlating noise and coming up with an erroneous source azimuth. On the other hand, a large number of sensors adds to the operational problems. For localizing a source emitting one watt at 7 Hz a 6 to 10 dB signal-to-noise enhancement would be desirable, and this would require at least four on-ice sensors in each linear element of the array.

The only benefit from a single linear array is indication of whether a quasi-stationary acoustic source is present in the vicinity. The square of the summed and delayed sensor outputs is given by two terms analytically, one of which is the covariance between sensor outputs. As Clay (1961) showed, in a dispersive medium the time delays between sensor outputs that yield a maximum covariance cannot be used to estimate source azimuth. However, if these delay increments change slowly and systematically over a fairly long period of time, the likelihood of a quasi-stationary source (submarine) would be suggested.

With some reservations we point out that source localization in a noisy, dispersive medium is possible if we were to ignore phase relations and only the signal intensity outputs from many geophones arrayed over a wide area

around a suspected source. It was illustrated graphically in the preceding sections that the phase velocity dispersion of acoustic signals gives rise to a signal intensity that falls off with range in an oscillatory manner. Thus, the signal intensities sensed by just a few widely spaced geophones near a submarine are not accurate indicators of the source position: a larger signal intensity might be sensed at a site farther from the source than at one closer. Moreover, the noise intensity and the non-uniformity of noise intensity would add to the uncertainty. However, if we were to "trap" the source within a closely spaced network of many sensors we could use a comparison of individual sensor outputs to identify the source position. This is a sledge hammer approach.

The approach is less demanding on the number of geophones where the source position is constrained by natural geographic barriers—such as the ice-covered waters of the Canadian Archipelago. There, access routes for a submarine are limited in places to deep water channels, and the number of geophones becomes the square root of the number required to yield the same coverage in an unbounded environment.

The Use of On-Ice Sensors Other than Geophones

Although the use of geophones has been emphasized in this report, we recognize that a wide variety of transducer types exist for the detection of small ice vibrations, e.g., piezoelectric and magnetostrictic sensors. These transducers are normally used to measure high-frequency vibration (above 10 kHz) whereas we have focused on the low-frequency sensitive geophone. However, in view of the unfavorable ratio predicted between the signal from ship-generated noise and natural ice vibration noise at low frequencies, we are prompted to discuss briefly the potential use of the high-frequency sensitive transducers.

A high-frequency sonar signal might be transmitted from the submarine for detecting dangerous under-ice protuberances. Because these sonar signals are above 1 kHz the total rate of signal attenuation due to spreading, absorption, refraction into ice, and scattering from the rough ice under-surface will be much greater than for the low frequencies previously discussed.

However, the unfavorable attenuation is offset by two important factors: the natural vibration amplitudes decrease with increasing frequency, and the acoustic power output of the sonar transducer is much larger than the power in spectral lines from submarine hydrodynamic, flow, and machinery noise sources.

To our knowledge natural ice vibration studies have not yet been made above 1 kHz. However, if the Knudsen noise curves indicate the variation of ice noise with frequency, then the noise amplitudes could be 20 to 40 dB below the noise level for the 10- to 100-Hz bandwidth.

The potential use of high-frequency on-ice transducers is an intriguing subject but the calculation of high frequency signal vibrations is not tractable to a simple analytical study such as given in this report: the short wavelengths of acoustic energy above 1 kHz pose greater complexity to the estimation of vibration amplitudes than at lower frequencies.

Conclusions and Recommendations

The studies reported here indicate that below 100 Hz ambient ice noise in the central Arctic Ocean results in a generally unfavorable signal-to-noise state for the on-ice detection of a nearby submarine. In the 1 to 10-Hz range the noise amplitudes are reported to be a minimum, and it is suggested that a submarine emitting a significant amount of power (one-watt) at 7 or 8 Hz would produce, within a 20 or 25 km radius from the source, a vibrational signal in the ice roughly equal to the amplitude of the maximum noise vibration. From 10 to 100 Hz the natural ice vibrations are uniformly large and the likely noise amplitudes are sufficient to overwhelm the signal from a nearby source emitting one-watt at discrete frequencies.

These conclusions are based on numerically derived signal amplitudes for a point source in an acoustical environment approximating the central Arctic Ocean, and on natural ice vibration noise measurements reported for the central Arctic Ocean.

The noise data used are from observations made during the late winter months. We would expect the natural vibrations to be lower during summer

months when the ice becomes "fluidized" and a poorer generator of seismic-acoustic noise, and thus the noise data used represent a worst noise state for the central Arctic Ocean. This state is most pertinent to the study for it corresponds to the season when the ice is thickest and leads fewest, consequently when hydrophone use is most severely restricted.

A literature search showed that noise vibrations have not been systematically measured in Arctic ice that covers shallow-water regions. This is unfortunate for the noise spectra may not be identical in both deep- and shallow-water regions. Nevertheless, signal amplitudes were also calculated for point sources in an idealized shallow-water acoustical environment with a water depth of 100 meters. At frequencies below about 50 Hz the calculated signal amplitudes at short ranges (< 15 km) are as much as 20 dB larger in shallow water than in deep water. This difference is caused by the stronger excitation of normal mode vibrations in the shallow water. However, above 50 Hz the ice-roughness attenuation of acoustic waves in shallow-water regions offsets the stronger excitation of the waves.

If the ice vibration noise above 5 Hz is caused principally by local disturbances occurring in and propagating through the ice, than the noise levels could be roughly the same in both environments. With this assumption the signal-to-noise ratio from 5 to 50 Hz might be 20 dB better at short ranges in shallow water than in the central Arctic Ocean. Thus, the on-ice transducer which seems to have at best marginal value in deep-water detection might be extremely effective for shallow-water detection of submarines. Whether this is true can only be determined from future ice vibration studies in shallow-water regions of the Arctic.

From tests in the central Arctic Ocean it has been shown that the hydrophone is much more effective in detecting underwater sound sources than the geophone. Comparisons of signals observed by means of the two transducers show a 10 to 40 dB signal-to-noise improvement with the hydrophone. This is explained by the noise waveguide behavior of the ice layer; the ice traps much of the vibrational energy generated within it. Consequently, a hydrophone must be preferred over an on-ice transducer whenever an alternative exists.

When there is no choice but to use an on-ice transducer the transducer used should have maximum sensitivity over the bandwidth of maximum signal-to-noise ratio. Ambient noise is a minimum from 2 to 10 Hz, and submarine generated acoustic signals might be relatively large in this frequency range. Therefore, a geophone with a resonant frequency from 2.0 to 7.5 Hz is suggested for on-ice sensing in deep Arctic waters.

Despite the generally unfavorable signal-to-noise ratio and dispersion of the signals, geophones can theoretically be used in two-dimensional arrays for estimating source azimuth. However, since one hundred or more transducers are necessary the operational problems of deploying, monitoring and processing the geophone outputs would be severe. Essentially, the same can be said for hydrophone operation. Although the signal-to-noise ratio of the hydrophone output should be better, the signal sought is still dispersive and two-dimensional hydrophone arrays are necessary for source localization.

Existing data concerned with natural ice noise is grossly inadequate. Experimental work as follows is therefore recommended.

Ice noise should be measured on ice over water less than 100 meters deep.

The frequency range should be from 1 Hz to the frequencies of submarine sonar. However, the emphasis should be on the frequencies between 1 Hz and 50 Hz.

These measurements, particularly the low frequency ones, should be made with three-component geophones. Sound waves from sources within the ice layer are likely to have important horizontal components as well as vertical components, whereas waves originating in the water are likely to have primarily vertical components in the ice.

Measurements of ice noise should be carried out to the extent that some statistical data are developed regarding the variation of ice noise from quiet days to stormy days.

APPENDIX A

Determination of the Eigen Wavenumbers

It was shown by Tolstoy (1956, 1958) that the characteristic equation for the eigen wavenumbers of totally reflected guided waves could be expressed in terms of phase angles $\chi\uparrow$ and $\chi\downarrow$ for the up-going and down-going waves. If the acoustical environment is approximated by n homogeneous layers, the characteristic equation is

$$e^{2i\chi\uparrow} \cdot e^{2i\chi\downarrow} \cdot e^{2ik_{mz}h_1} = 1$$

or

$$\chi\uparrow + \chi\downarrow + k_{mz}h_1 = m\pi$$

where m is an integer, the mode number; k_{mz} is the vertical component of the eigen wavenumber, the parameter that also satisfies the phase integral; and h_1 is the thickness of the low velocity layer. If the upper boundary is a free surface, then $\chi\uparrow = 0$ and the characteristic equation reduces to

$$\chi\downarrow + k_{mz}h_1 = m\pi \qquad \text{(A.1)}$$

To solve for the eigen wavenumbers we must expand $\chi\downarrow$ in terms of the entire acoustical system. In the Arctic Ocean the sonic velocity, α, increases monotonically with depth. Partitioning the environment into n layers, and assuming no partial reflections, total reflection will occur at the i, (i + 1) is interface where the phase velocity of the guided wave, c, $\alpha_i<c<\alpha_{i+1}$ (α_i and α_{i+1} are the acoustic velocities in the (i + 1) layers, respectively). At this interface the resulting phase change is

$$\chi_{i,i+1} = \tan^{-1}\left(p_{i,i+1}\frac{\rho_{i+1}}{\rho_i}\right)$$

where

$$p_{i,i+1} = \left\{\frac{c^2 - \alpha^2_{i+1}}{\alpha_i^2 - c^2\left(\frac{\alpha_2}{\alpha_{i+1}}\right)^2}\right\}^{1/2}$$

and ρ_i, ρ_{i+1} are the densities of the i and (i + 1) layers, respectively (Brekhovskikh, 1960). In the simplest of all cases, a single low velocity layer over a half space (i = 1), we find that $\chi\!\downarrow = \chi_{i,i+1}$ and for a given c we may solve explicitly for the k_{mz}. However, when we consider a less trivial case in which the down-going waves penetrate more than one layer, the determination of k_{mz} becomes less direct. Each layer above the reflecting interface will affect the total phase change experienced by the wave. In this case $\chi\!\downarrow$ can be found through the recursive relationships given:

$$\chi\!\downarrow = \tan^{-1}\left[p_{12}\frac{\rho_2}{\rho_1}\tan\left(\gamma_2 h_2 + \chi_{23}\right)\right]$$

$$\chi_{23} = \tan^{-1}\left[p_{23}\frac{\rho_3}{\rho_2}\tan\left(\gamma_3 h_3 + \chi_{34}\right)\right]$$

$$\chi_{n-1,n} = \tan^{-1}\left[p_{n-1,n}\frac{\rho_n}{\rho_{n-1}}\tan\left(\gamma_n h_n + \chi_{n,n+1}\right)\right]$$

$$\chi_{n,n+1} = \tan^{-1}\left[p_{n,n+1}\frac{\rho_{n+1}}{\rho_n}\right] \qquad \text{(A.2)}$$

where γ is the magnitude of the eigen wavenumber in the i - th layer,

$$\gamma_i = k\left[1 - \left(\frac{\alpha_i}{c}\right)^2\right]^{1/2} = \frac{\omega}{c}\left[1 - \left(\frac{\alpha_1}{c}\right)^2\right]^{1/2}$$

To solve for k_{mz}, Tolstoy (1955) gives an iterative method easily adapted to high-speed machine evaluation.

APPENDIX B

The Effect of Ice Roughness on the Guided Waves

If we consider a harmonic wave with amplitude A_m and wavenumber k_{mz}* incident at a rough or irregular sea water-sea ice boundary, then the reflection will not be entirely specular. A portion of the incident energy will be reflected in directions whose corresponding wavenumbers no longer satisfy the condition for unattenuated guided waves. This energy is not trapped in the guide and attenuates rapidly. Assuming the ice thickness to be small compared to the wavelength of the incident wave and the surface to have a Gaussian distribution function, then total reflection of the incident wave occurs; but the amplitude specularly reflected portion is (Clay, 1964)

$$A_m' \simeq A_m e^{-2(k_{mz}\sigma)^2}$$

where the random surface $\zeta(x)$ is characterized by the distribution function

$$D(\zeta) = \frac{1}{\sigma(2\pi)^{1/2}} \exp(-\zeta^2/2\sigma^2)$$

Because k_{mz} is dependent on the mode, different modes will suffer different rates of attenuation. In general k_{mz} increases with mode, and hence the lowest modes should contribute most to the signal at long ranges.

In a waveguide distance R the wave will suffer n reflections. If the thickness of the guide is h, the number of reflections is

$$n = R/2h \tan\theta_m$$

*As before we define k_{mz} as the vertical component of the eigen wavenumber.

where θ_m is the angle of incidence for the m-th mode. Thus if A_m is the unattenuated amplitude, the attenuated amplitude, $A_m'(R)$ after waveguide distance travel R becomes

$$A_m'(R) = A_m e^{-2n(k_{mz}\sigma)^2}$$

or

$$A_m'(R) = A_m e^{-\gamma_m R}$$

where

$$\gamma_m = \frac{k_{mz}}{k_{mr}h}(k_{mz}\sigma)^2$$

and

$$k^2 = k_{mz}^2 + k_{mr}^2$$

When more than a single mode is involved the ice roughness will also modify the signal intensity at distance R by causing an incoherence of the modes relative to each other. In Eq. 7 it was shown that the signal intensity is derived in part from a term expressing the phase interaction of the modes. This term has a dependence on range R like

$$\cos\,(k_{mr} - k_{nr})R$$

However, in a waveguide of changing thickness neither k_{mz} nor k_{mr} are constant, these eigenvalues change slightly with perturbations in the height of the ice bottom irregularities. Clay (1964) states that $\cos(k_{mr} - k_{nr})R$ must be replaced by a term derived from averaging $\cos(k_{mr} - k_{mz})R$ over the Gaussian distribution, $D(\zeta)$. Thus, the phase interaction term is shown to vary with range like

$$(\exp\{-(k_{mr} - k_{nr})\}^2 R^2\sigma^2/2h^2)\,\cos\,(k_{mr} - k_{nr})R$$

BIBLIOGRAPHY

Brekhovskikh, L.M. (1960) Waves in layered media, Academic Press, New York.

Brune, J. and J. Oliver (1959) The seismic noise of the earth's surface, Bull. Seismo. Soc. Am., v. 49, p. 349-353.

Clay, C.S. (1961) Array steering in a layered waveguide, Jour. Acous. Soc. Am., v. 33, n. 7, p. 865,870.

Clay, C.S. (1964) Effect of a slightly irregular boundary on the coherence of waveguide propagation, Jour. Acous. Soc. Am., v. 36, n. 5, p. 833-837.

Eckart, C. (1953) The scattering of sound from the sea surface, Jour. Acous. Soc. Am., v. 25, p. 566-570; Sea surface, Jour. Acous. Soc. Am., v. 25, p. 566-570.

Ewing, M., C.L. Pekeris, and Worzel, J.L. (1948) Propagation of sound in the Ocean, Geol. Soc. Am., Memoir 27.

Goldstein, N.E. (1966) Seismometers on Arctic ice for detection of underwater acoustic disturbances, Tech. Report 2, Project ETU-2167-612, Naval Warfare Research Center, Stanford Research Institute, Menlo Park, California.

Greene, C.R., T.F. Elbert, and M.U. Fitzpatrick (1966) Phase I of Arctic Airborne ASW System Study (U); General Motors Research Defense Lab. (S, Group 3).

Hunkins, K. (1960) Seismic studies of sea ice, Jour. Geoph. Res., v.67, p. 2477-2489.

Millen, R.H. and H.W. Marsh (1965) Underwater sound in the Arctic Ocean, Report MED-65-1002, AVCO Marine Electronics Office.

Milne, A.R., and S.R. Clark (1964) Resonances in seismic noise under Arctic sea-ice, Bull. Seismological Soc. Am., v. 54, n. 6, p. 1797-1809.

Milne, A.R. and T.H. Ganton (1964) Ambient Noise under Arctic sea-ice, Jour. Acous. Soc. Am., v. 36, p. 855-863.

Officer, C.B. (1958) Introduction to the theory of sound transmission with application to the ocean, McGraw-Hill, New York

Pekeris, C.L. (1948) Theory of propagation of explosive sound in shallow water, Geol. Soc. Am., Memoir 27, 117 p.

Prentiss, D., E. Davis, and H. Kutschale (1965) Natural and man-made vibrations in the Central Arctic Ocean in the frequency range from 0.1 to 100 cps, Tech. Rep. 4, CU-4-65, Lamong Geological Obs.

Press, F. and W.F. Brace (1966) Earthquake prediction, Science v. 152, 17 June

Press, F. and M. Ewing (1951) Propagation of elastic waves in a floating ice sheet, Trans. Am. Geoph. Un., v. 32, n. 5.

Tolstoy, I. (1955) Dispersion and simple harmonic point sources in wave ducts, Jour. Acous. Soc. Am., v. 27, p. 897-907.

Tolstoy, I. (1958) Shallow water test of the theory of layered waves guides, Jour. Acous. Soc. Am., v. 30, p. 348-361.

CONFIDENTIAL
Security Classification

DOCUMENT CONTROL DATA - R&D

(Security classification of title, body of abstract and indexing annotation must be entered when the overall report is classified)

1. ORIGINATING ACTIVITY (Corporate author)	2a. REPORT SECURITY CLASSIFICATION
Naval Warfare Research Center Stanford Research Institute Menlo Park, California	CONFIDENTIAL 2b GROUP 4

3 REPORT TITLE

THE APPLICATION OF SEISMOMETERS TO ARCTIC ASW—AN ANALYTICAL STUDY

4 DESCRIPTIVE NOTES (Type of report and inclusive dates)

Technical Report

5 AUTHOR(S) (Last name, first name, initial)

Norman E. Goldstein

6. REPORT DATE	7a. TOTAL NO. OF PAGES	7b. NO. OF REFS
February 1967	56	19

8a. CONTRACT OR GRANT NO.	9a. ORIGINATOR'S REPORT NUMBER(S)
Nonr-2332(00)	SRI 66-3252 2167-612
b PROJECT NO. RF-018-02	
c. RF-018-02-06	9b. OTHER REPORT NO(S) (Any other numbers that may be assigned this report)
d. NR-274-008	Technical Report

10. AVAILABILITY/LIMITATION NOTICES

In addition to security requirements which must be met, this document is subject to special export controls and each transmittal to foreign governments or foreign nationals may be made only with prior approval of Office of Naval Research (Code 462)

11. SUPPLEMENTARY NOTES	12. SPONSORING MILITARY ACTIVITY
	Naval Ordnance Laboratory White Oak Silver Spring, Maryland

13. ABSTRACT

In ice-covered waters the usefulness of hydrophones is limited by the necessity to create or to locate openings through which the sensors can enter the water. But ability to detect submarines in Arctic waters is important. For this reason the effectiveness of an on-ice sensor, namely, the geophone, has been studied analytically toward the assessment of its feasibility. Comparisons were made between meager measurements of ice noise reported in the literature and signal levels calculated from normal mode theory. The studies indicate that a submarine emitting one-watt or more at 7 or 8 Hz, a frequency range of low natural noise, might be detectable at a range of 1 km and possibly as large as 30 km.

Noise data is lacking particularly for shallow water areas, where the geophone seems most useful, and experimental measurements are recommended using three component geophones.

No matter what the signal-to-noise ratio, array processing can be used to enhance the probability of recognizing a submarine. However, the acoustic environment causes dispersive waves and this would add to the operational difficulties.

DD FORM 1 JAN 64 1473

CONFIDENTIAL
Security Classification

CONFIDENTIAL

Security Classification

14. KEY WORDS	LINK A		LINK B		LINK C	
	ROLE	WT	ROLE	WT	ROLE	WT
Seismometers						
Arctic						
ASW						
Analytical Study						

INSTRUCTIONS

1. ORIGINATING ACTIVITY: Enter the name and address of the contractor, subcontractor, grantee, Department of Defense activity or other organization *(corporate author)* issuing the report.

2a. REPORT SECURITY CLASSIFICATION: Enter the overall security classification of the report. Indicate whether "Restricted Data" is included. Marking is to be in accordance with appropriate security regulations.

2b. GROUP: Automatic downgrading is specified in DoD Directive 5200.10 and Armed Forces Industrial Manual. Enter the group number. Also, when applicable, show that optional markings have been used for Group 3 and Group 4 as authorized.

3. REPORT TITLE: Enter the complete report title in all capital letters. Titles in all cases should be unclassified. If a meaningful title cannot be selected without classification, show title classification in all capitals in parenthesis immediately following the title.

4. DESCRIPTIVE NOTES: If appropriate, enter the type of report, e.g., interim, progress, summary, annual, or final. Give the inclusive dates when a specific reporting period is covered.

5. AUTHOR(S): Enter the name(s) of author(s) as shown on or in the report. Enter last name, first name, middle initial. If military, show rank and branch of service. The name of the principal author is an absolute minimum requirement.

6. REPORT DATE: Enter the date of the report as day, month, year; or month, year. If more than one date appears on the report, use date of publication.

7a. TOTAL NUMBER OF PAGES: The total page count should follow normal pagination procedures, i.e., enter the number of pages containing information.

7b. NUMBER OF REFERENCES: Enter the total number of references cited in the report.

8a. CONTRACT OR GRANT NUMBER: If appropriate, enter the applicable number of the contract or grant under which the report was written.

8b, 8c, & 8d. PROJECT NUMBER: Enter the appropriate military department identification, such as project number, subproject number, system numbers, task number, etc.

9a. ORIGINATOR'S REPORT NUMBER(S): Enter the official report number by which the document will be identified and controlled by the originating activity. This number must be unique to this report.

9b. OTHER REPORT NUMBER(S): If the report has been assigned any other report numbers *(either by the originator or by the sponsor)*, also enter this number(s).

10. AVAILABILITY/LIMITATION NOTICES: Enter any limitations on further dissemination of the report, other than those imposed by security classification, using standard statements such as:

(1) "Qualified requesters may obtain copies of this report from DDC."

(2) "Foreign announcement and dissemination of this report by DDC is not authorized."

(3) "U. S. Government agencies may obtain copies of this report directly from DDC. Other qualified DDC users shall request through ________________."

(4) "U. S. military agencies may obtain copies of this report directly from DDC. Other qualified users shall request through ________________."

(5) "All distribution of this report is controlled. Qualified DDC users shall request through ________________."

If the report has been furnished to the Office of Technical Services, Department of Commerce, for sale to the public, indicate this fact and enter the price, if known.

11. SUPPLEMENTARY NOTES: Use for additional explanatory notes.

12. SPONSORING MILITARY ACTIVITY: Enter the name of the departmental project office or laboratory sponsoring *(paying for)* the research and development. Include address.

13. ABSTRACT: Enter an abstract giving a brief and factual summary of the document indicative of the report, even though it may also appear elsewhere in the body of the technical report. If additional space is required, a continuation sheet shall be attached.

It is highly desirable that the abstract of classified reports be unclassified. Each paragraph of the abstract shall end with an indication of the military security classification of the information in the paragraph, represented as *(TS)*, *(S)*, *(C)*, or *(U)*.

There is no limitation on the length of the abstract. However, the suggested length is from 150 to 225 words.

14. KEY WORDS: Key words are technically meaningful terms or short phrases that characterize a report and may be used as index entries for cataloging the report. Key words must be selected so that no security classification is required. Identifiers, such as equipment model designation, trade name, military project code name, geographic location, may be used as key words but will be followed by an indication of technical context. The assignment of links, roles, and weights is optional.

DD FORM 1 JAN 64 1473 (BACK)

CONFIDENTIAL

Security Classification